Eur. Phys. J. C (2019) 79:444
https://doi.org/10.1140/epjc/s10052-019-6926-x

THE EUROPEAN PHYSICAL JOURNAL C

Regular Article - Experimental Physics

Search for supersymmetry in events with a photon, jets, b-jets, and missing transverse momentum in proton–proton collisions at 13 TeV

CMS Collaboration*

CERN, 1211 Geneva 23, Switzerland

Received: 20 January 2019 / Accepted: 3 May 2019 / Published online: 25 May 2019

Abstract A search for supersymmetry is presented based on events with at least one photon, jets, and large missing transverse momentum produced in proton–proton collisions at a center-of-mass energy of 13 TeV. The data correspond to an integrated luminosity of 35.9 fb^{-1} and were recorded at the LHC with the CMS detector in 2016. The analysis characterizes signal-like events by categorizing the data into various signal regions based on the number of jets, the number of b-tagged jets, and the missing transverse momentum. No significant excess of events is observed with respect to the expectations from standard model processes. Limits are placed on the gluino and top squark pair production cross sections using several simplified models of supersymmetric particle production with gauge-mediated supersymmetry breaking. Depending on the model and the mass of the next-to-lightest supersymmetric particle, the production of gluinos with masses as large as 2120 GeV and the production of top squarks with masses as large as 1230 GeV are excluded at 95% confidence level.

1 Introduction

The standard model (SM) of particle physics successfully describes many phenomena, but lacks several necessary elements to provide a complete description of nature, including a source for the relic abundance of dark matter (DM) [1,2] in the universe. In addition, the SM must resort to fine tuning [3–6] to explain the hierarchy between the Planck mass scale and the electroweak scale set by the vacuum expectation value of the Higgs field, the existence of which was recently confirmed by the observation of the Higgs boson (H) [7,8]. Supersymmetry (SUSY) [9–16] is an extension of the SM that can provide both a viable DM candidate and additional particles that inherently cancel large quantum corrections to the Higgs boson mass-squared term from the SM fields.

Supersymmetric models predict a bosonic superpartner for each SM fermion and a fermionic superpartner for each SM boson; each new particle's spin differs from that of its SM partner by half a unit. SUSY also includes a second Higgs doublet. New colored states, such as gluinos ($\widetilde{\text{g}}$) and top squarks ($\widetilde{\text{t}}$), the superpartners of the gluon and the top quark, respectively, are expected to have masses on the order of 1 TeV to avoid fine tuning in the SM Higgs boson mass-squared term. In models that conserve R-parity [17], each superpartner carries a conserved quantum number that requires superpartners to be produced in pairs and causes the lightest SUSY particle (LSP) to be stable. The stable LSP can serve as a DM candidate.

The signatures targeted in this paper are motivated by models in which gauge-mediated SUSY breaking (GMSB) is responsible for separating the masses of the SUSY particles from those of their SM counterparts. In GMSB models, the gaugino masses are expected to be proportional to the size of their fundamental couplings. This includes the superpartner of the graviton, the gravitino ($\widetilde{\text{G}}$), whose mass is proportional to $M_{\text{SB}}/M_{\text{Pl}}$, where M_{SB} represents the scale of the SUSY breaking interactions and M_{Pl} is the Planck scale where gravity is expected to become strong. GMSB permits a significantly lower symmetry-breaking scale than, e.g., gravity mediation, and therefore generically predicts that the $\widetilde{\text{G}}$ is the LSP [18–20], with a mass often much less than 1 GeV. Correspondingly, the next-to-LSP (NLSP) is typically a neutralino, a superposition of the superpartners of the neutral bosons. The details of the quantum numbers of the NLSP play a large part in determining the phenomenology of GMSB models, including the relative frequencies of the Higgs bosons, Z bosons, and photons produced in the NLSP decay.

The scenario of a natural SUSY spectrum with GMSB and R-parity conservation typically manifests as events with multiple jets, at least one photon, and large $p_{\text{T}}^{\text{miss}}$, the magnitude of the missing transverse momentum. Depending on the topology, these jets can arise from either light-flavored

* e-mail: cms-publication-committee-chair@cern.ch

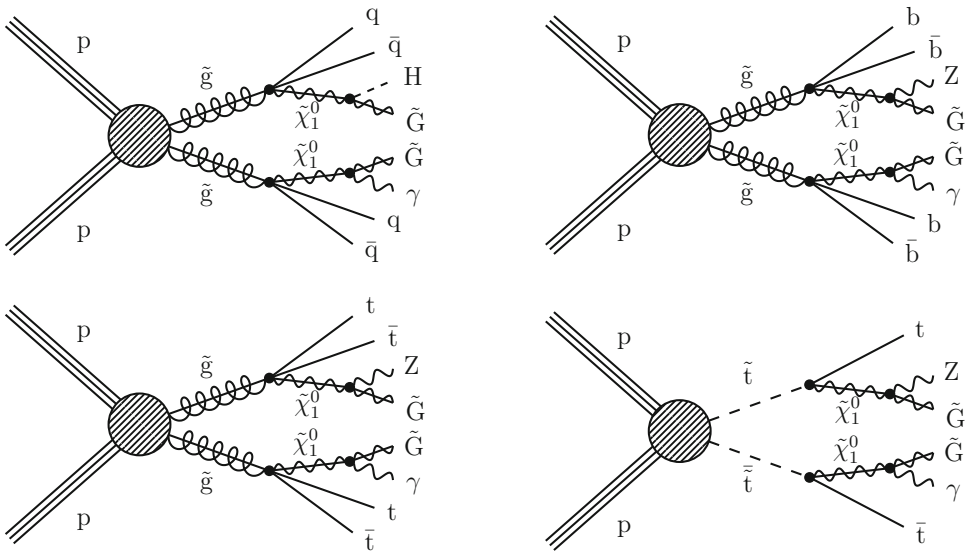

Fig. 1 Example diagrams depicting the simplified models used, which are defined in the text. The top left diagram depicts the T5qqqqHG model, the top right diagram depicts the T5bbbbZG model, the bottom left diagram depicts the T5ttttZG model, and the bottom right depicts the T6ttZG model

quarks (u, d, s, c) or b quarks. We study four simplified models [21–25]; example diagrams depicting these models are shown in Fig. 1. Three models involve gluino pair production (prefixed with T5), and one model involves top squark pair production (prefixed with T6). In the T5qqqqHG model, each gluino decays to a pair of light-flavored quarks ($q\bar{q}$) and a neutralino ($\widetilde{\chi}_1^0$). The T5bbbbZG and T5ttttZG models are similar to T5qqqqHG, except that the each pair of light-flavored quarks is replaced by a pair of bottom quarks ($b\bar{b}$) or a pair of top quarks ($t\bar{t}$), respectively. In the T5qqqqHG model, the $\widetilde{\chi}_1^0$ decays either to an SM Higgs boson and a $\widetilde{G}$ or to a photon and a $\widetilde{G}$. The $\widetilde{\chi}_1^0 \to H\widetilde{G}$ branching fraction is assumed to be 50%, and the smallest $\widetilde{\chi}_1^0$ mass considered is 127 GeV. In the T5bbbbZG and T5ttttZG models, the neutralinos decay to $Z\widetilde{G}$ and $\gamma\widetilde{G}$ with equal probability. The T6ttZG model considers top squark pair production, with each top squark decaying into a top quark and a neutralino. The neutralino can then decay with equal probability to a photon and a $\widetilde{G}$ or to a Z boson and a $\widetilde{G}$. For the models involving the decay $\widetilde{\chi}_1^0 \to Z\widetilde{G}$, we probe $\widetilde{\chi}_1^0$ masses down to 10 GeV. All decays of SUSY particles are assumed to be prompt. In all models, the mass $m_{\widetilde{G}}$ is fixed to be 1 GeV, to be consistent with other published results. For the parameter space explored here, the kinematic properties do not depend strongly on the exact value of $m_{\widetilde{G}}$.

The proton–proton (pp) collision data used in this search correspond to an integrated luminosity of 35.9 fb^{-1} and were collected with the CMS detector during the 2016 run of the CERN LHC [26]. Signal-like events with at least one photon are classified into signal regions depending on the number of jets N_{jets}, the number of tagged bottom quark jets $N_{\text{b-jets}}$, and the $p_{\text{T}}^{\text{miss}}$. The expected yields from SM backgrounds are estimated using a combination of simulation and data control regions. We search for gluino or top squark pair production as an excess of observed data events compared to the expected background yields.

Previous searches for R-parity conserving SUSY with photons in the final state performed by the CMS Collaboration are documented in Refs. [27,28]. Similar searches have also been performed by the ATLAS Collaboration [29–31]. This work improves on the previous results by identifying jets from b quarks, which can be produced by all of the signal models shown in Fig. 1. We also include additional signal regions that exploit high jet multiplicities for sensitivity to high-mass gluino models, and we rely more on observed data for the background estimations. These improvements enable us to explore targeted signal models that produce b quarks in the final state and are expected to improve sensitivity to the models explored in Refs. [27–31].

In this paper, a description of the CMS detector and simulation used are presented in Sect. 2. The event reconstruction and signal region selections are presented in Sect. 3. The methods used for predicting the SM backgrounds are presented in Sect. 4. Results are given in Sect. 5. The analysis is summarized in Sect. 6.

2 Detector and simulation

A detailed description of the CMS detector, along with a definition of the coordinate system and pertinent kinematic variables, is given in Ref. [32]. Briefly, a cylindrical superconducting solenoid with an inner diameter of 6 m provides a 3.8 T axial magnetic field. Within the cylindrical volume are a silicon pixel and strip tracker, a lead tungstate crystal electromagnetic calorimeter (ECAL), and a brass and scintillator hadron calorimeter (HCAL). The tracking detectors cover the pseudorapidity range $|\eta| < 2.5$. The ECAL and

HCAL, each composed of a barrel and two endcap sections, cover $|\eta| < 3.0$. Forward calorimeters extend the coverage to $3.0 < |\eta| < 5.0$. Muons are detected within $|\eta| < 2.4$ by gas-ionization detectors embedded in the steel flux-return yoke outside the solenoid. The detector is nearly hermetic, permitting accurate measurements of $p_{\mathrm{T}}^{\mathrm{miss}}$. The CMS trigger is described in Ref. [33].

Monte Carlo (MC) simulation is used to design the analysis, to provide input for background estimation methods that use data control regions, and to predict event rates from simplified models. Simulated SM background processes include jets produced through the strong interaction, referred to as quantum chromodynamics (QCD) multijets, $\mathrm{t\bar{t}}$+jets, W+jets, Z+jets, γ+jets, $\mathrm{t\bar{t}}\gamma$, $\mathrm{t}\gamma$, and Vγ+jets (V = Z, W). The SM background events are generated using the MadGraph5_aMC@NLO v2.2.2 or v2.3.3 generator [34–36] at leading order (LO) in perturbative QCD, except $\mathrm{t\bar{t}}\gamma$ and $\mathrm{t}\gamma$, which are generated at next-to-leading order (NLO). The cross sections used for normalization are computed at NLO or next-to-NLO [34,37–39]. The QCD multijets, diboson (Vγ), top quark, and vector boson plus jets events are generated with up to two, two, three, and four additional partons in the matrix element calculations, respectively. Any duplication of events between pairs of related processes – QCD multijets and γ+jets; $\mathrm{t\bar{t}}$+jets and $\mathrm{t\bar{t}}\gamma$; W+jets and Wγ+jets– is removed using generator information.

The NNPDF3.0 [40] LO (NLO) parton distribution functions (PDFs) are used for samples simulated at LO (NLO). Parton showering and hadronization are described using the pythia 8.212 generator [41] with the CUETP8M1 underlying event tune [42]. Partons generated with MadGraph5_aMC@NLO and pythia that would otherwise be counted twice are removed using the MLM [43] and FxFx [44] matching schemes in LO and NLO samples, respectively.

Signal samples are simulated at LO using the MadGraph5_aMC@NLO v2.3.3 generator and their yields are normalized using NLO plus next-to-leading logarithmic (NLL) cross sections [45–49]. The decays of gluinos, top squarks, and neutralinos are modeled with pythia.

The detector response to particles produced in the simulated collisions is modeled with the Geant4 [50] detector simulation package for SM processes. Because of the large number of SUSY signals considered, with various gluino, squark, and neutralino masses, the detector response for these processes is simulated with the CMS fast simulation [51,52]. The results from the fast simulation generally agree with the results from the full simulation. Where there is disagreement, corrections are applied, most notably a correction of up to 10% to adjust for differences in the modeling of $p_{\mathrm{T}}^{\mathrm{miss}}$.

3 Event reconstruction and selection

The CMS particle-flow (PF) algorithm [53] aims to reconstruct every particle in each event, using an optimal combination of information from all detector systems. Particle candidates are identified as charged hadrons, neutral hadrons, electrons, photons, or muons. For electron and photon PF candidates, further requirements are applied to the ECAL shower shape and the ratio of associated energies in the ECAL and HCAL [54,55]. Similarly, for muon PF candidates, further requirements are applied to the matching between track segments in the silicon tracker and the muon detectors [56]. These further requirements improve the quality of the reconstruction. Electron and muon candidates are restricted to $|\eta| < 2.5$ and < 2.4, respectively. The $p_{\mathrm{T}}^{\mathrm{miss}}$ is calculated as the magnitude of the negative vector p_{T} sum of all PF candidates.

After all interaction vertices are reconstructed, the primary pp interaction vertex is selected as the vertex with the largest p_{T}^2 sum of all physics objects. The physics objects used in this calculation are produced by a jet-finding algorithm [57,58] applied to all charged-particle tracks associated to the vertex, plus the corresponding $p_{\mathrm{T}}^{\mathrm{miss}}$ computed from those jets. To mitigate the effect of secondary pp interactions (pileup), charged-particle tracks associated with vertices other than the primary vertex are not considered for jet clustering or calculating object isolation sums.

Jets are reconstructed by clustering PF candidates using the anti-k_{T} jet algorithm [57,58] with a size parameter of 0.4. To eliminate spurious jets, for example those induced by electronics noise, further jet quality criteria [59] are applied. The jet energy response is corrected for the nonlinear response of the detector [60]. There is also a correction to account for the expected contributions of neutral particles from pileup, which cannot be removed based on association with secondary vertices [61]. Jets are required to have $p_{\mathrm{T}} > 30\,\mathrm{GeV}$ and are restricted to be within $|\eta| < 2.4$. The combined secondary vertex algorithm (CSVv2) at the medium working point [62] is applied to each jet to determine if it should be identified as a bottom quark jet. The CSVv2 algorithm at the specified working point has a 55% efficiency to correctly identify b jets with $p_{\mathrm{T}} \approx 30\,\mathrm{GeV}$. The corresponding misidentification probabilities are 1.6% for gluon and light-flavor quark jets, and 12% for charm quark jets.

Photons with $p_{\mathrm{T}} > 100\,\mathrm{GeV}$ and $|\eta| < 2.4$ are used in this analysis, excluding the ECAL transition region with $1.44 < |\eta| < 1.56$. To suppress jets erroneously identified as photons from neutral hadron decays, photon candidates are required to be isolated. An isolation cone of radius $\Delta R = \sqrt{(\Delta\phi)^2 + (\Delta\eta)^2} < 0.2$ is used, with no dependence on the p_{T} of the photon candidate. Here, ϕ is the azimuthal angle in radians. The energy measured in the isolation cone is corrected for contributions from pileup [61].

The shower shape and the fractions of hadronic and electromagnetic energy associated with the photon candidate are required to be consistent with expectations from prompt photons. The candidates matched to a track measured by the pixel detector (pixel seed) are rejected because they are likely to result from electrons that produced electromagnetic showers.

Similarly, to suppress jets erroneously identified as leptons and genuine leptons from hadron decays, electron and muon candidates are also subjected to isolation requirements. The isolation variable I is computed from the scalar p_{T} sum of selected charged hadron, neutral hadron, and photon PF candidates, divided by the lepton p_{T}. PF candidates enter the isolation sum if they satisfy $R < R_I(p_{\mathrm{T}})$. The cone radius R_I decreases with lepton p_{T} because the collimation of the decay products of the parent particle of the lepton increases with the Lorentz boost of the parent [63]. The values used are $R_I = 0.2$ for $p_{\mathrm{T}}^{\ell} < 50\,\mathrm{GeV}$, $R_I = 10\,\mathrm{GeV}/p_{\mathrm{T}}^{\ell}$ for $50 \leq p_{\mathrm{T}}^{\ell} \leq 200\,\mathrm{GeV}$, and $R_I = 0.05$ for $p_{\mathrm{T}}^{\ell} > 200\,\mathrm{GeV}$, where $\ell = \mathrm{e}, \mu$. As with photons, the expected contributions from pileup are subtracted from the isolation variable. The isolation requirement is $I < 0.1$ (0.2) for electrons (muons).

We additionally veto events if they contain PF candidates which are identified as an electron, a muon, or a charged hadron, and satisfy an isolation requirement computed using tracks. Isolated hadronic tracks are common in background events with a tau lepton that decays hadronically. The track isolation variable I_{track} is computed for each candidate from the scalar p_{T} sum of selected other charged-particle tracks, divided by the candidate p_{T}. Other charged-particle tracks are selected if they lie within a cone of radius 0.3 around the candidate direction and come from the primary vertex. The isolation variable must satisfy $I_{\mathrm{track}} < 0.2$ for electrons and muons, and $I_{\mathrm{track}} < 0.1$ for charged hadrons. Isolated tracks are required to satisfy $|\eta| < 2.4$, and the transverse mass of each isolated track with $p_{\mathrm{T}}^{\mathrm{miss}}$, $m_{\mathrm{T}} = \sqrt{2 p_{\mathrm{T}}^{\mathrm{track}} p_{\mathrm{T}}^{\mathrm{miss}} (1 - \cos\Delta\phi)}$ where $\Delta\phi$ is the difference in ϕ between $\vec{p}_{\mathrm{T}}^{\,\mathrm{track}}$ and $\vec{p}_{\mathrm{T}}^{\,\mathrm{miss}}$, is required to be less than 100 GeV.

Signal event candidates were recorded by requiring a photon at the trigger level with a requirement $p_{\mathrm{T}}^{\gamma} > 90\,\mathrm{GeV}$ if $H_{\mathrm{T}}^{\gamma} = p_{\mathrm{T}}^{\gamma} + \Sigma p_{\mathrm{T}}^{\mathrm{jet}} > 600\,\mathrm{GeV}$ and $p_{\mathrm{T}}^{\gamma} > 165\,\mathrm{GeV}$ otherwise. These quantities are computed at the trigger level. The efficiency of this trigger, as measured in data, is $(98 \pm 2)\%$ after applying the selection criteria described below. Additional triggers, requiring the presence of charged leptons, photons, or minimum $H_{\mathrm{T}} = \Sigma p_{\mathrm{T}}^{\mathrm{jet}}$, are used to select control samples employed in the evaluation of backgrounds.

Signal-like candidate events must fulfill one of two requirements, based on the trigger criteria described above: $p_{\mathrm{T}}^{\gamma} > 100\,\mathrm{GeV}$ and $H_{\mathrm{T}}^{\gamma} > 800\,\mathrm{GeV}$, or $p_{\mathrm{T}}^{\gamma} > 190\,\mathrm{GeV}$ and $H_{\mathrm{T}}^{\gamma} > 500\,\mathrm{GeV}$. In addition to these requirements, the events should have at least 2 jets and $p_{\mathrm{T}}^{\mathrm{miss}} > 100\,\mathrm{GeV}$. To reduce backgrounds from the SM processes that produce a leptonically decaying W boson, resulting in $p_{\mathrm{T}}^{\mathrm{miss}}$ from the undetected neutrino, events are rejected if they have any charged light leptons (e, μ) with $p_{\mathrm{T}} > 10\,\mathrm{GeV}$ or any isolated electron, muon, or charged hadron tracks with $p_{\mathrm{T}} > 5, 5, 10\,\mathrm{GeV}$, respectively. Events from the γ+jets process typically satisfy the above criteria when the energy of a jet is mismeasured, inducing artificial $p_{\mathrm{T}}^{\mathrm{miss}}$. To reject these events, the two highest p_{T} jets are both required to have an angular separation from the $p_{\mathrm{T}}^{\mathrm{miss}}$ direction in the transverse plane, $\Delta\phi_{1,2} > 0.3$. Events with reconstruction failures, detector noise, or beam halo interactions are rejected using dedicated identification requirements [64].

The selected events are divided into 25 exclusive signal regions, also called signal bins, based on $p_{\mathrm{T}}^{\mathrm{miss}}$, the number of jets N_{jets}, and the number of b-tagged jets $N_{\text{b-jets}}$. The signal regions can be grouped into 6 categories based on N_{jets} and $N_{\text{b-jets}}$, whose intervals are defined to be N_{jets}: 2–4, 5–6, $\geq$7; and $N_{\text{b-jets}}$: 0, $\geq$1. Within each of the 6 categories, events are further distinguished based on 4 exclusive regions, defined as: $200 < p_{\mathrm{T}}^{\mathrm{miss}} < 270$, $270 < p_{\mathrm{T}}^{\mathrm{miss}} < 350$, $350 < p_{\mathrm{T}}^{\mathrm{miss}} < 450$, and $p_{\mathrm{T}}^{\mathrm{miss}} > 450\,\mathrm{GeV}$. In the lowest N_{jets}, $N_{\text{b-jets}}$ category, the highest $p_{\mathrm{T}}^{\mathrm{miss}}$ bin is further subdivided into two intervals: $450 < p_{\mathrm{T}}^{\mathrm{miss}} < 750\,\mathrm{GeV}$ and $p_{\mathrm{T}}^{\mathrm{miss}} > 750\,\mathrm{GeV}$. Events with $100 < p_{\mathrm{T}}^{\mathrm{miss}} < 200\,\mathrm{GeV}$ are used as a control region for estimating SM backgrounds. These categories in N_{jets}, $N_{\text{b-jets}}$, and $p_{\mathrm{T}}^{\mathrm{miss}}$ were found to provide good sensitivity to the various signal models described above, while minimizing uncertainties in the background predictions.

4 Background estimation

There are four main mechanisms by which SM processes can produce events with the target signature of a photon, multiple jets, and $p_{\mathrm{T}}^{\mathrm{miss}}$. These mechanisms are: (1) the production of a high-p_{T} photon along with a W or Z boson that decays leptonically, and either any resulting electron or muon is "lost" (lost-lepton) or any resulting τ lepton decays hadronically (τ_{h}); (2) the production of a W boson that decays to eν and the electron is misidentified as a photon; (3) the production of a high-p_{T} photon in association with a Z boson that decays to neutrinos; and (4) the production of a photon along with a jet that is mismeasured, inducing high $p_{\mathrm{T}}^{\mathrm{miss}}$. QCD multijet events with a jet misidentified as a photon and a mismeasured jet do not contribute significantly to the SM background.

The total event yield from each source of background is estimated separately for each of the 25 signal regions. The methods and uncertainties associated with the background predictions are detailed in the following sections.

4.1 Lost-lepton and τ_{h} backgrounds

The lost-lepton background arises from events in which the charged lepton from a leptonically decaying W boson, pro-

duced directly or from the decay of a top quark, cannot be identified. This can occur because the lepton is out of acceptance, fails the identification requirements, or fails the isolation requirements. For example, in events with high-p_T top quarks, the top quark decay products will be collimated, forcing the b jet to be closer to the charged lepton. In this case, the lepton is more likely to fail the isolation requirements. This background is estimated by studying control regions in both data and simulation, obtained by requiring both a well-identified photon and a light lepton (e, μ). For every signal region, there are two lost lepton control regions that have the exact same definition as the signal region except either exactly one electron or exactly one muon is required.

The τ_h background arises from events in which a W boson decays to a τ lepton, which subsequently decays to mesons and a neutrino. These hadronic decays of τ leptons occur approximately 65% of the time. Because of lepton universality, the fraction of events with τ_h candidates can be estimated from the yield of events containing a single muon, after correcting for the reconstruction differences and for the τ_h branching fraction.

The lost-lepton and τ_h background predictions rely on an extrapolation between eγ or $\mu\gamma$ event yields and single photon event yields. In all control regions where a single light lepton is required, the dominant SM processes that contribute are Wγ and t$\bar{\text{t}}\gamma$. Lost-muon and hadronic tau events are estimated using $\mu\gamma$ control regions, while lost-electron events are estimated using eγ control regions. In each control region, exactly one electron or muon is required and the isolated track veto for the selected lepton flavor is removed. In order to reduce the effect of signal contamination and to increase the fraction of SM events in the control sample, events are only selected if the m_T of the lepton-p_T^{miss} system is less than 100 GeV. In SM background events with a single lepton and p_T^{miss}, the m_T of the system is constrained by the mass of the W boson; this is not the case for signal events, because of the presence of gravitinos. All other kinematic variable requirements for each signal region are applied to the corresponding control regions.

Transfer factors are derived using simulated Wγ+jets and t$\bar{\text{t}}\gamma$ processes, which determine the average number of events expected in the signal region for each eγ or $\mu\gamma$ event observed in the control region. The Zγ events in which the Z boson decays leptonically have a negligible contribution to the transfer factors. The transfer factors applied to the $\mu\gamma$ control regions account for both lost-μ events and τ_h events. They are denoted by the symbol $T_{\mu,\tau}$ and are typically in the range $0.7 < T_{\mu,\tau} < 1.0$. The transfer factors applied to eγ events account for only the lost-e events. They are denoted by the symbol T_e and are typically in the range $0.3 < T_e < 0.6$. The transfer factors are parameterized versus N_{jets}, $N_{b\text{-jets}}$, and p_T^{miss}; however, for $p_T^{miss} > 150$ GeV, T_ℓ is found to be independent of p_T^{miss}. The parameterization of the transfer

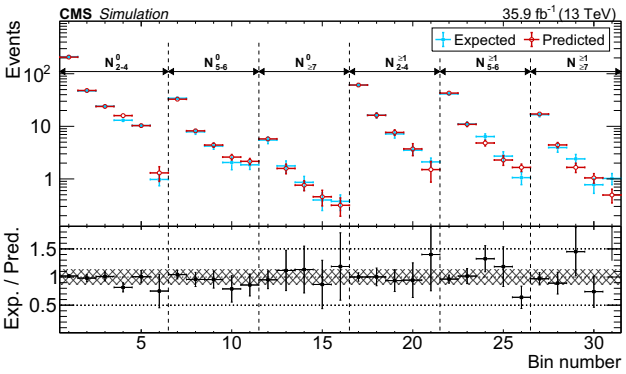

Fig. 2 The lost-lepton and τ_h event yields as predicted directly from simulation in the signal regions, shown in red, and from the prediction procedure applied to simulated eγ or $\mu\gamma$ events, shown in blue. The error bars correspond to the statistical uncertainties from the limited number of events in simulation. The bottom panel shows the ratio of the simulation expectation (Exp.) and the simulation-based prediction (Pred.). The hashed area shows the expected uncertainties from data-to-simulation correction factors, PDFs, and renormalization and factorization scales. The categories, denoted by dashed lines, are labeled as N_j^b, where j refers to the number of jets and b refers to the number of b-tagged jets. The numbered bins within each category are the various p_T^{miss} bins. In each of these regions, the first bin corresponds to $100 < p_T^{miss} < 200$ GeV, which belongs to a control region. The remaining bins correspond to the signal regions in Table 1

factors is validated using simulation by treating eγ or $\mu\gamma$ events like data and comparing the predicted lost-lepton and τ_h event yields to the true simulated event yields in the signal regions. This comparison is shown in Fig. 2. The prediction in each signal region is $N_\ell^{pred} = \Sigma_i N_i T_{\ell,i}$, where $\ell = e, \mu$ and i ranges from 1 to n, where n is the number of transfer factors that contribute in a given signal region.

The dominant uncertainty in the lost-lepton background predictions arises from the limited numbers of events in the eγ and $\mu\gamma$ control regions. These uncertainties are modeled in the final statistical interpretations as a gamma distribution whose shape parameter is set by the observed number of events and whose scale parameter is the average transfer factor for that bin. Other systematic uncertainties in the determination of the transfer factors include the statistical uncertainty from the limited number of simulated events, which is typically 5–10% but can be as large as 20%, as well as uncertainties in the jet energy corrections, PDFs, renormalization (μ_R) and factorization (μ_F) scales, and simulation correction factors. The uncertainties in μ_R and μ_F are obtained by varying each value independently by factors of 0.5 and 2.0 [65,66]. Simulation correction factors are used to account for differences between the observed data and modeling of b-tagging efficiencies, b jet misidentification, and lepton reconstruction efficiencies in simulation. One of the largest uncertainties, apart from the statistical uncertainty in the data control regions and the simulation, comes from

mismodeling of photons which are collinear with electrons, which has a 12% effect on the lost-lepton prediction.

4.2 Misidentified photon background

Events containing the decay $W \to e\nu$ are the primary source of electrons that are erroneously identified as photons. Photon misidentification can occur when a pixel detector seed fails to be associated with the energy deposit in the ECAL. Given a misidentification rate, which relates events with an erroneously identified photon to events with a well-identified electron, the photon background can be estimated from a single-electron (zero-photon) control region. The misidentification rate is estimated in simulation and corrections are derived from observed data to account for any mismodeling in simulation.

The single-electron control regions are defined by the same kinematic requirements as the single-photon signal regions, except that we require no photons and exactly one electron, and we use the momentum of the electron in place of the momentum of the photon for photon-based variables. As explained in the previous section, in addition to all of the signal region selections, events are required to satisfy $m_{\mathrm{T}}(\mathrm{e}, p_{\mathrm{T}}^{\mathrm{miss}}) < 100\,\mathrm{GeV}$.

To extrapolate from the event yields in the single-electron control regions to the event yields for the misidentified photon background in the signal regions, we derive a misidentification rate $f = N_\gamma/N_{\mathrm{e}}$ using a combination of simulation and data. The misidentification rate is determined as a function of the electron p_{T} and the multiplicity Q_{mult} of charged-particle tracks from the primary vertex in a region around the electron candidate. The charged-track multiplicity is computed by counting the number of charged PF candidates (electrons, muons, hadrons) in the jet closest to the electron candidate. If there is no jet within $\Delta R < 0.3$ of the electron candidate, Q_{mult} is set to zero. A typical event in the single-electron control region has a Q_{mult} of 3–4. The electron p_{T} and Q_{mult} dependence of the misidentification rate is derived using simulated W+jets and $\mathrm{t\bar{t}}$+jets events. The misidentification rate is on average 1–2%, but can be as low as 0.5% for events with high Q_{mult}.

To account for systematic differences between the misidentification rates in data and simulation, we correct the misidentification rate by measuring it in both simulated and observed Drell–Yan (DY) events. Separate corrections are derived for low Q_{mult} ($\leq$1) and high Q_{mult} ($\geq$2). The DY control region is defined by requiring one electron with $p_{\mathrm{T}} > 40\,\mathrm{GeV}$ and another reconstructed particle, either a photon or an oppositely charged electron, with $p_{\mathrm{T}} > 100\,\mathrm{GeV}$. A further requirement $50 < (m_{\mathrm{e^+e^-}}\ \mathrm{or}\ m_{\mathrm{e}\gamma}) < 130\,\mathrm{GeV}$ is applied to ensure the particles are consistent with the decay products of a Z boson, and therefore the photon is likely to be a misidentified electron. The misidentification rate is computed as the ratio $N_{\mathrm{e}\gamma}/N_{\mathrm{e^+e^-}}$, where $N_{\mathrm{e}\gamma}$ ($N_{\mathrm{e^+e^-}}$) is the number of events in the $\mathrm{e}\gamma$ ($\mathrm{e^+e^-}$) control region. It is found to be 15–20% higher in data than in simulation.

The prediction of the misidentified-photon background in the signal region is then given by the weighted sum of the observed events in the control region, where the weight is given by the data-corrected misidentification rate for photons. The dominant uncertainty in the prediction is a 14% uncertainty in the data-to-simulation correction factors, followed by the uncertainty in the limited number of events in the simulation at large values of $p_{\mathrm{T}}^{\mathrm{miss}}$. The misidentified-photon background prediction also includes uncertainties in the modeling of initial-state radiation (ISR) in the simulation, statistical uncertainties from the limited number of events in the data control regions, uncertainties in the pileup modeling, and uncertainties in the trigger efficiency measurement.

4.3 Background from $\mathrm{Z}(\nu\bar{\nu})\gamma$ events

Decays of the Z boson to invisible particles constitute a major background for events with low N_{jets}, low $N_{\mathrm{b\text{-}jets}}$, and high $p_{\mathrm{T}}^{\mathrm{miss}}$. The $\mathrm{Z}(\nu\bar{\nu})\gamma$ background is estimated using $\mathrm{Z}(\ell^+\ell^-)\gamma$ events. The shape of the distribution of $p_{\mathrm{T}}^{\mathrm{miss}}$ vs. N_{jets} in $\mathrm{Z}(\nu\bar{\nu})\gamma$ events is modeled in simulation, while the normalization and the purity of the control region are measured in data.

Events in the $\ell^+\ell^-\gamma$ control region are required to have exactly two oppositely charged, same-flavor leptons (ℓ = e or μ) and one photon with $p_{\mathrm{T}} > 100\,\mathrm{GeV}$. The dilepton invariant mass $m_{\ell\ell}$ is required to be consistent with the Z boson mass, $80 < m_{\ell\ell} < 100\,\mathrm{GeV}$. The charged leptons serve as a proxy for neutrinos, so the event-level kinematic variables, such as $p_{\mathrm{T}}^{\mathrm{miss}}$, are calculated after removing charged leptons from the event.

The $\ell^+\ell^-\gamma$ control region may contain a small fraction of events from processes other than $\mathrm{Z}(\ell^+\ell^-)\gamma$, primarily $\mathrm{t\bar{t}}\gamma$. We define the purity of the control region as the percentage of events originating from the $\mathrm{Z}(\ell^+\ell^-)\gamma$ process. The purity is computed in data by measuring the number of events in the corresponding oppositely charged, different-flavor control region, which has a higher proportion of $\mathrm{t\bar{t}}\gamma$ events. The purity is found to be $(97 \pm 3)\%$. A statistically compatible purity is also measured in the oppositely charged, same-flavor control region. In this region, the $m_{\ell\ell}$ distribution is used to extrapolate from the number of events with $m_{\ell\ell}$ far from the Z boson mass to the number of events with $m_{\ell\ell}$ close to it.

The $\mathrm{Z}(\nu\bar{\nu})\gamma$ predictions from simulation are scaled to the total $\mathrm{Z}(\ell^+\ell^-)\gamma$ yield observed according to $N_{\mathrm{Z}(\nu\bar{\nu})\gamma} = \beta R_{\nu\nu/\ell\ell} N_{\mathrm{Z}(\ell^+\ell^-)\gamma}$, where β is the purity of the $\mathrm{Z}(\ell^+\ell^-)\gamma$ control region and $R_{\nu\nu/\ell\ell}$ is the ratio between the expected number of $\mathrm{Z}(\nu\bar{\nu})\gamma$ and $\mathrm{Z}(\ell^+\ell^-)\gamma$ events. The ratio $R_{\nu\nu/\ell\ell}$, which accounts for lepton reconstruction effects and the rel-

ative branching fractions for $Z \to \nu\bar{\nu}$ and $Z \to \ell^+\ell^-$, is determined from simulation.

The primary uncertainty in the $Z(\nu\bar{\nu})\gamma$ prediction arises from uncertainties in the p_T^{miss} distribution from the simulation. Other uncertainties include statistical uncertainties from the limited number of events in the simulation and uncertainties in the estimation of the control region purity. The p_T^{γ}-dependent NLO electroweak corrections [67] are assigned as additional uncertainties to account for any mismodeling of the photon p_T in simulation. This uncertainty has a magnitude of 8% for the lowest p_T^{miss} bin and rises to 40% for $p_T^{miss} > 750\,GeV$.

4.4 Background from γ+jets events

The γ+jets background is dominated by events in which a genuine photon is accompanied by an energetic jet with mismeasured p_T, resulting in high p_T^{miss}. The QCD multijet events with a jet misidentified as a photon and a mismeasured jet contribute to this background at a much smaller rate; these events are measured together with events from the γ+jets process. Most of these events are removed by requiring that the azimuthal angles between the $\vec{p}_T^{\,miss}$ and each of the two highest p_T jets satisfy $\Delta\phi_{1,2} > 0.3$. Inverting this requirement provides a large control region of low-$\Delta\phi$ events that is used to predict the γ+jets background in the signal regions. The ratio of high-$\Delta\phi$ events to low-$\Delta\phi$ events, $R_{h/l}$, is derived from the low-p_T^{miss} sideband ($100 < p_T^{miss} < 200\,GeV$).

While most of the events in both the low-$\Delta\phi$ and the low-p_T^{miss} control regions are γ+jets events, electroweak backgrounds in which p_T^{miss} arises from W or Z bosons decaying to one or more neutrinos, like those discussed previously, will contaminate these control regions. The contamination can be significant for high N_{jets} and $N_{b\text{-}jets}$, where $t\bar{t}$ events are more prevalent. The rates of these events in the control regions are predicted using the same techniques, as discussed in the previous sections.

A double ratio $\kappa = R_{h/l}^{p_T^{miss}>200\,GeV} / R_{h/l}^{p_T^{miss}<200\,GeV}$ is derived from simulated γ+jets events in order to account for the dependence of $R_{h/l}$ on p_T^{miss}. To test how well the simulation models κ, we use a zero-photon validation region in which the contribution from events containing a mismeasured jet dominates. To be consistent with the trigger used to select the data in this region, these events are also required to have $H_T > 1000\,GeV$. Electroweak contamination in the zero-photon validation region is estimated using simulated Vγ+jets (V = Z, W), $t\bar{t}\gamma$, $t\bar{t}$+jets, W+jets, and $Z(\nu\bar{\nu})$+jets events. The comparison of κ in data and simulation is shown in Fig. 3. The level of disagreement is found to be less than 20%.

Event yields for the γ+jets background are computed from the high-p_T^{miss}, low-$\Delta\phi$ control regions according to

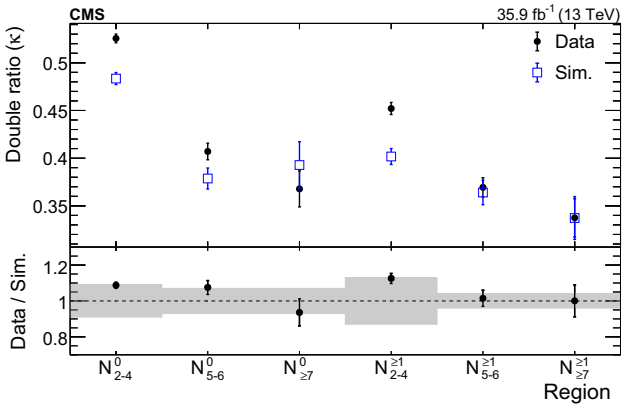

Fig. 3 The double ratio κ in each N_{jets}-$N_{b\text{-}jets}$ region for zero-photon events. The filled black circles are the observed κ values after subtracting the electroweak contamination based on simulation. The open blue squares are the κ values computed directly from simulation. The ratio is shown in the bottom panel, where the shaded region corresponds to the systematic uncertainty in the γ+jets prediction. In the label N_j^b, j refers to the number of jets and b refers to the number of b-tagged jets

$N_{\gamma+jets} = \kappa N_{low\text{-}\Delta\phi} R_{h/l}$. $N_{low\text{-}\Delta\phi}$ is the event yield in the high-p_T^{miss}, low-$\Delta\phi$ control region after removing contributions from electroweak backgrounds.

Uncertainties in the γ+jets prediction are dominated by the statistical uncertainties either from the limited number of events in the low-$\Delta\phi$ control regions or from the predictions of the electroweak contamination. The <20% disagreement between the κ values in data and simulation in the zero-photon validation region is included as an additional uncertainty. Uncertainties in the b-tagging correction factors are a minor contribution to the uncertainty in the γ+jets prediction.

5 Results and interpretations

The predicted background and observed yields are shown in Table 1 and Fig. 4. The largest deviation is found in bin 2 ($2 \le N_{jets} \le 4$, $N_{b\text{-}jets} = 0$, and $270 < p_T^{miss} < 350\,GeV$), where the background is predicted to be 91 events with 51 events observed. The local significance of this single bin was computed to be around 2 standard deviations below the SM expectation. This calculation does not account for the look-elsewhere effect associated with the use of 25 exclusive signal regions, which is expected to reduce this significance. In general, a large deviation in a single bin is inconsistent with the expected distributions of events from the signal models considered here. The observations in all other bins are consistent with the SM expectations within one standard deviation.

Limits are evaluated for the production cross sections of the signal scenarios discussed in Sect. 1 using a maximum likelihood fit for the SUSY signal strength, the yields of the five classes of background events shown in Fig. 4, and various

Table 1 Predicted and observed event yields for each of the 25 exclusive signal regions

N_{jets}	$N_{\text{b-jets}}$	$p_{\text{T}}^{\text{miss}}$ (GeV)	Lost e	Lost $\mu + \tau_{\text{h}}$	Misid. γ	$\text{Z}(\nu\overline{\nu})\gamma$	γ+jets	Total	Data
2–4	0	200–270	10.5 ± 2.6	31.2 ± 6.0	22.3 ± 5.4	33.6 ± 8.3	60 ± 11	157 ± 16	151
2–4	0	270–350	5.8 ± 1.8	29.6 ± 5.9	11.9 ± 2.9	22.9 ± 6.0	20.5 ± 4.3	91 ± 10	51
2–4	0	350–450	1.68 ± 0.88	13.9 ± 3.9	6.6 ± 1.6	17.0 ± 5.2	4.1 ± 1.4	43.3 ± 6.8	50
2–4	0	450–750	1.98 ± 0.94	8.1 ± 3.1	6.7 ± 1.5	18.1 ± 7.1	2.5 ± 1.3	37.4 ± 8.0	33
2–4	0	> 750	$0.00^{+0.69}_{-0.00}$	1.2 ± 1.2	0.79 ± 0.19	2.8 ± 1.2	$0.41^{+0.42}_{-0.41}$	5.2 ± 1.9	6
5–6	0	200–270	1.28 ± 0.61	5.1 ± 1.9	3.53 ± 0.75	3.09 ± 0.78	15.8 ± 4.8	28.8 ± 5.3	26
5–6	0	270–350	2.06 ± 0.80	3.2 ± 1.5	2.39 ± 0.56	1.98 ± 0.54	3.7 ± 1.8	13.3 ± 2.6	11
5–6	0	350–450	0.77 ± 0.46	$0.64^{+0.65}_{-0.64}$	1.26 ± 0.30	1.49 ± 0.47	1.23 ± 0.97	5.4 ± 1.4	8
5–6	0	> 450	0.26 ± 0.26	1.9 ± 1.1	1.00 ± 0.24	1.65 ± 0.65	$0.07^{+0.52}_{-0.07}$	4.9 ± 1.4	7
≥ 7	0	200–270	$0.00^{+0.61}_{-0.00}$	$0.0^{+1.3}_{-0.0}$	0.72 ± 0.16	0.37 ± 0.11	1.8 ± 1.2	2.9 ± 1.9	3
≥ 7	0	270–350	$0.34^{+0.35}_{-0.34}$	1.5 ± 1.0	0.38 ± 0.10	0.24 ± 0.08	1.22 ± 0.94	3.6 ± 1.5	3
≥ 7	0	350–450	$0.34^{+0.35}_{-0.34}$	0.73 ± 0.73	0.17 ± 0.05	0.16 ± 0.07	$0.07^{+0.50}_{-0.07}$	1.46 ± 0.96	0
≥ 7	0	> 450	$0.00^{+0.61}_{-0.00}$	$0.0^{+1.3}_{-0.0}$	0.20 ± 0.06	0.17 ± 0.08	$0.00^{+0.75}_{-0.00}$	$0.37^{+1.60}_{-0.37}$	0
2–4	≥ 1	200–270	3.4 ± 1.5	14.5 ± 4.2	7.1 ± 1.7	3.55 ± 0.89	11.3 ± 3.3	39.8 ± 5.9	50
2–4	≥ 1	270–350	2.9 ± 1.4	5.6 ± 2.5	3.79 ± 0.92	2.45 ± 0.65	5.7 ± 1.8	20.4 ± 3.6	20
2–4	≥ 1	350–450	$0.0^{+1.0}_{-0.0}$	1.1 ± 1.1	2.00 ± 0.45	1.81 ± 0.55	0.59 ± 0.44	5.5 ± 1.7	4
2–4	≥ 1	> 450	2.3 ± 1.2	4.4 ± 2.3	1.62 ± 0.38	2.14 ± 0.84	0.95 ± 0.54	11.5 ± 2.8	8
5–6	≥ 1	200–270	3.5 ± 1.3	2.4 ± 1.4	5.5 ± 1.2	0.76 ± 0.20	7.7 ± 2.4	19.9 ± 3.3	21
5–6	≥ 1	270–350	1.06 ± 0.64	4.0 ± 1.8	2.98 ± 0.63	0.49 ± 0.14	2.1 ± 1.0	10.6 ± 2.3	15
5–6	≥ 1	350–450	0.71 ± 0.51	2.4 ± 1.4	1.38 ± 0.29	0.32 ± 0.11	$0.30^{+0.49}_{-0.30}$	5.1 ± 1.6	6
5–6	≥ 1	> 450	$0.35^{+0.36}_{-0.35}$	$0.0^{+1.4}_{-0.0}$	0.67 ± 0.15	0.48 ± 0.20	$0.00^{+0.56}_{-0.00}$	$1.5^{+1.6}_{-1.5}$	2
≥ 7	≥ 1	200–270	0.72 ± 0.53	2.0 ± 1.2	1.68 ± 0.37	0.13 ± 0.04	5.9 ± 5.0	10.5 ± 5.1	12
≥ 7	≥ 1	270–350	$0.00^{+0.65}_{-0.00}$	1.33 ± 0.96	0.73 ± 0.16	0.10 ± 0.04	$0.0^{+1.1}_{-0.0}$	2.2 ± 1.6	1
≥ 7	≥ 1	350–450	0.72 ± 0.53	$0.0^{+1.2}_{-0.0}$	0.44 ± 0.10	0.07 ± 0.03	$0.0^{+1.1}_{-0.0}$	$1.2^{+1.7}_{-1.2}$	1
≥ 7	≥ 1	> 450	$0.36^{+0.37}_{-0.36}$	$0.0^{+1.2}_{-0.0}$	0.23 ± 0.07	0.04 ± 0.02	$0.0^{+1.1}_{-0.0}$	$0.6^{+1.7}_{-0.6}$	1

nuisance parameters. The SUSY signal strength μ is defined to be the ratio of the observed signal cross section to the predicted cross section. A nuisance parameter refers to a variable not of interest in this search, such as the effect of parton distribution function uncertainties in a background prediction. The nuisance parameters are constrained by observed data in the fit. The uncertainties in the predicted signal yield arise from the uncertainties in renormalization and factorization scales, ISR modeling, jet energy scale, b-tagging efficiency and misidentification rate, corrections to simulation, limited numbers of simulated events, and the integrated luminosity measurement [26]. The largest uncertainty comes from the ISR modeling; it ranges from 4 to 30% depending on the signal region and the signal parameters, taking higher values for regions with large N_{jets} or for signals with $\Delta m \approx 0$. Here, Δm is the difference in mass between the gluino or squark and its decay products, e.g. $\Delta m = m_{\tilde{\text{g}}} - (m_{\tilde{\chi}_1^0} + 2m_{\text{t}})$ for the T5ttttZG model when on-shell top quarks are produced. The second-largest uncertainty comes from the correction for differences between GEANT4 and the fast simulation in $p_{\text{T}}^{\text{miss}}$ modeling, with a maximum value of 10%. The procedures used to evaluate the systematic uncertainties in the signal predictions in the context of this search are described in Ref. [68].

For the models of gluino pair production considered here, the limits are derived as a function of $m_{\tilde{\text{g}}}$ and $m_{\tilde{\chi}_1^0}$, while for the model of top squark pair production, the limits are a function of $m_{\tilde{\text{t}}}$ and $m_{\tilde{\chi}_1^0}$. The likelihood used for the statistical interpretation models the yield in each of the signal regions as a Poisson distribution, multiplied by constraints which account for the uncertainties in the background predictions and signal yields. For the predictions in which an observed event yield in a control region is scaled, a gamma distribution is used to model the Poisson uncertainty of the observed control region yield. All other uncertainties are modeled as log-normal distributions. The test statistic is $q_\mu = -2 \ln \mathcal{L}_\mu / \mathcal{L}_{\text{max}}$, where $\mathcal{L}_{\text{max}}$ is the maximum likelihood determined by leaving all parameters as free, including the signal strength, and $\mathcal{L}_\mu$ is the maximum likelihood for a fixed value of μ. Limits are determined

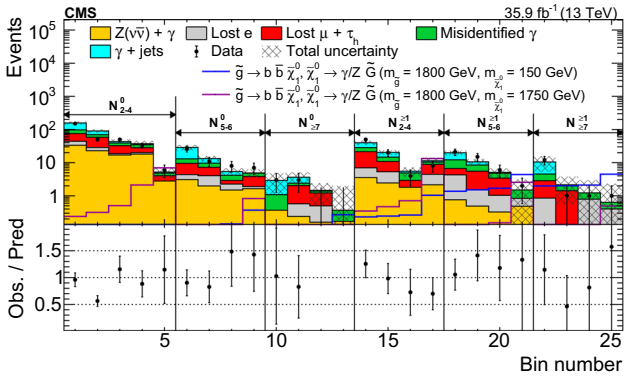

Fig. 4 Observed numbers of events and predicted numbers of events from the various SM backgrounds in the 25 signal regions. The categories, denoted by vertical lines, are labeled as $N_{\mathrm{j}}^{\mathrm{b}}$, where j refers to the number of jets and b refers to the number of b-tagged jets. The numbered bins within each category are the various $p_{\mathrm{T}}^{\mathrm{miss}}$ bins, as defined in Table 1. The lower panel shows the ratio of the observed events to the predicted SM background events. The error bars in the lower panel are the quadrature sum of the statistical uncertainty in the observed data and the systematic uncertainty in the predicted backgrounds before the adjustments based on a maximum likelihood fit to data assuming no signal strength

using an approximation of the asymptotic form of the test statistic distribution [69] in conjunction with the $\mathrm{CL_s}$ criterion [70,71]. Expected upper limits are derived by varying observed yields according to the expectations from the background-only hypothesis.

Using the statistical procedure described above, 95% confidence level (CL) upper limits are computed on the signal cross section for each simplified model and each mass hypothesis. Exclusion limits are defined by comparing observed upper limits to the predicted NLO+NLL signal cross section. The signal cross sections are also varied according to theoretical uncertainties to give a ± 1 standard deviation variation on the observed exclusion contour. The 95% CL cross section limits and exclusion contours for the four models considered, T5qqqqHG, T5bbbbZG, T5ttttZG, and T6ttZG, are shown in Fig. 5.

Generally, the limits degrade at both high and low $m_{\widetilde{\chi}_1^0}$. For $m_{\widetilde{\chi}_1^0} \approx m_{\widetilde{\mathrm{g}}}\,(m_{\widetilde{\mathrm{t}}})$, the quarks from the decay of gluinos (top squarks) have low p_{T}. Correspondingly, the H_{T}^{γ}, N_{jets}, and $N_{\mathrm{b\text{-}jets}}$ distributions tend toward lower values, reducing the signal efficiency and causing signal events to populate regions with higher background yields. For small $m_{\widetilde{\chi}_1^0}$, the quarks produced in the decay of gluinos or top squarks have high p_{T} but lower $p_{\mathrm{T}}^{\mathrm{miss}}$ on average. For all models except T5qqqqHG, when the NLSP mass drops below the mass of the Z boson, the kinematics of the NLSP decay require the Z boson to be far off-shell. As the Z boson mass is forced to be lower, the LSP will carry a larger fraction of the momentum of the NLSP, producing larger $p_{\mathrm{T}}^{\mathrm{miss}}$. This causes a slight increase in the sensitivity when the NLSP mass is near the Z boson mass. While a similar effect would happen for the T5qqqqHG model, the simulation used here does not probe the region of parameter space where the Higgs boson would be forced to have a mass far off-shell. Similarly, the limits for top squark production improve slightly at very high $m_{\widetilde{\chi}_1^0}$, when the top quarks become off-shell. In this case, the $\widetilde{\chi}_1^0$ carries a larger fraction of the top squark momentum, increasing the $p_{\mathrm{T}}^{\mathrm{miss}}$.

For moderate $m_{\widetilde{\chi}_1^0}$, gluino masses as large as 2090, 2120, and 1970 GeV are excluded for the T5qqqqHG, T5bbbbZG, and T5ttttZG models, respectively. Top squark masses as large as 1230 GeV are excluded for the T6ttZG model. For small $m_{\widetilde{\chi}_1^0}$, gluino masses as large as 1920, 1950, and 1800 GeV are excluded for the T5qqqqHG, T5bbbbZG, and T5ttttZG models, respectively. Top squark masses as large as 1110 GeV are excluded for the T6ttZG model. There is close agreement between the observed and expected limits.

6 Summary

A search for gluino and top squark pair production is presented, based on a proton–proton collision dataset at a center-of-mass energy of 13 TeV recorded with the CMS detector in 2016. The data correspond to an integrated luminosity of $35.9\,\mathrm{fb}^{-1}$. Events are required to have at least one isolated photon with transverse momentum $p_{\mathrm{T}} > 100$ GeV, two jets with $p_{\mathrm{T}} > 30$ GeV and pseudorapidity $|\eta| < 2.4$, and missing transverse momentum $p_{\mathrm{T}}^{\mathrm{miss}} > 200$ GeV.

The data are categorized into 25 exclusive signal regions based on the number of jets, the number of b-tagged jets, and $p_{\mathrm{T}}^{\mathrm{miss}}$. Background yields from the standard model processes are predicted using simulation and data control regions. The observed event yields are found to be consistent with expectations from the standard model processes within the uncertainties.

Results are interpreted in the context of simplified models. Four such models are studied, three of which involve gluino pair production and one of which involves top squark pair production. All models assume a gauge-mediated supersymmetry (SUSY) breaking scenario, in which the lightest SUSY particle is a gravitino ($\widetilde{\mathrm{G}}$). We consider scenarios in which the gluino decays to a neutralino $\widetilde{\chi}_1^0$ and a pair of light-flavor quarks (T5qqqqHG), bottom quarks (T5bbbbZG), or top quarks (T5ttttZG). In the T5qqqqHG model, the $\widetilde{\chi}_1^0$ decays with equal probability either to a photon and a $\widetilde{\mathrm{G}}$ or to a Higgs boson and a $\widetilde{\mathrm{G}}$. In the T5bbbbZG and T5ttttZG models, the $\widetilde{\chi}_1^0$ decays with equal probability either to a photon and a $\widetilde{\mathrm{G}}$ or to a Z boson and a $\widetilde{\mathrm{G}}$. In the top squark pair production model (T6ttZG), top squarks decay to a top quark and $\widetilde{\chi}_1^0$, and the $\widetilde{\chi}_1^0$ decays with equal probability either to a photon and a $\widetilde{\mathrm{G}}$ or to a Z boson and a $\widetilde{\mathrm{G}}$.

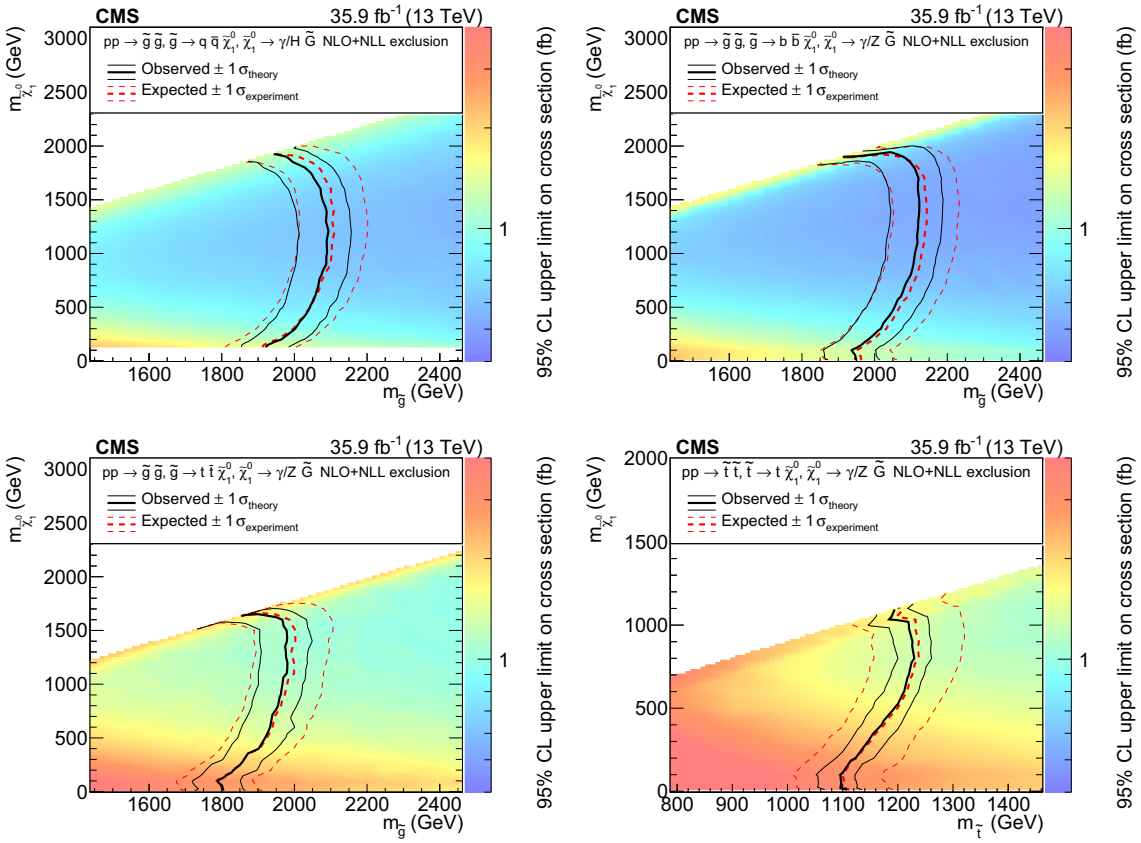

Fig. 5 Observed and expected 95% CL upper limits for gluino or top squark pair production cross sections for the T5qqqqHG (upper left), T5bbbbZG (upper right), T5ttttZG (bottom left), and T6ttZG (bottom right) models. Black lines denote the observed exclusion limit and the uncertainty due to variations of the theoretical prediction of the gluino or top squark pair production cross section. The dashed lines correspond to the region containing 68% of the distribution of the expected exclusion limits under the background-only hypothesis

Using the cross sections for SUSY pair production calculated at next-to-leading order plus next-to-leading logarithmic accuracy, we place 95% confidence level lower limits on the gluino mass as large as 2120 GeV, depending on the model and the $m_{\tilde{\chi}_1^0}$ value, and limits on the top squark mass as large as 1230 GeV, depending on the $m_{\tilde{\chi}_1^0}$ value. These results significantly improve upon those from previous searches for SUSY with photons.

Acknowledgements We congratulate our colleagues in the CERN accelerator departments for the excellent performance of the LHC and thank the technical and administrative staffs at CERN and at other CMS institutes for their contributions to the success of the CMS effort. In addition, we gratefully acknowledge the computing centers and personnel of the Worldwide LHC Computing Grid for delivering so effectively the computing infrastructure essential to our analyses. Finally, we acknowledge the enduring support for the construction and operation of the LHC and the CMS detector provided by the following funding agencies: BMBWF and FWF (Austria); FNRS and FWO (Belgium); CNPq, CAPES, FAPERJ, FAPERGS, and FAPESP (Brazil); MES (Bulgaria); CERN; CAS, MoST, and NSFC (China); COLCIENCIAS (Colombia); MSES and CSF (Croatia); RPF (Cyprus); SENESCYT (Ecuador); MoER, ERC IUT, and ERDF (Estonia); Academy of Finland, MEC, and HIP (Finland); CEA and CNRS/IN2P3 (France); BMBF, DFG, and HGF (Germany); GSRT (Greece); NKFIA (Hungary); DAE and DST (India); IPM (Iran); SFI (Ireland); INFN (Italy); MSIP and NRF (Republic of Korea); MES (Latvia); LAS (Lithuania); MOE and UM (Malaysia); BUAP, CINVESTAV, CONACYT, LNS, SEP, and UASLP-FAI (Mexico); MOS (Montenegro); MBIE (New Zealand); PAEC (Pakistan); MSHE and NSC (Poland); FCT (Portugal); JINR (Dubna); MON, RosAtom, RAS, RFBR, and NRC KI (Russia); MESTD (Serbia); SEIDI, CPAN, PCTI, and FEDER (Spain); MOSTR (Sri Lanka); Swiss Funding Agencies (Switzerland); MST (Taipei); ThEPCenter, IPST, STAR, and NSTDA (Thailand); TUBITAK and TAEK (Turkey); NASU and SFFR (Ukraine); STFC (United Kingdom); DOE and NSF (USA). Individuals have received support from the Marie-Curie program and the European Research Council and Horizon 2020 Grant, contract No. 675440 (European Union); the Leventis Foundation; the A. P. Sloan Foundation; the Alexander von Humboldt Foundation; the Belgian Federal Science Policy Office; the Fonds pour la Formation à la Recherche dans l'Industrie et dans l'Agriculture (FRIA-Belgium); the Agentschap voor Innovatie door Wetenschap en Technologie (IWT-Belgium); the F.R.S.-FNRS and FWO (Belgium) under the "Excellence of Science - EOS" - be.h project n. 30820817; the Ministry of Education, Youth and Sports (MEYS) of the Czech Republic; the Lendület ("Momentum") Programme and the János Bolyai Research Scholarship of the Hungarian Academy of Sciences, the New National Excellence Program ÚNKP, the NKFIA research Grants 123842, 123959, 124845, 124850 and 125105 (Hungary); the Council of Science and Industrial Research, India; the HOMING PLUS program of the Foun-

dation for Polish Science, cofinanced from European Union, Regional Development Fund, the Mobility Plus program of the Ministry of Science and Higher Education, the National Science Center (Poland), contracts Harmonia 2014/14/M/ST2/00428, Opus 2014/13/B/ST2/02543, 2014/15/B/ST2/03998, and 2015/19/B/ST2/02861, Sonata-bis 2012/07/E/ST2/01406; the National Priorities Research Program by Qatar National Research Fund; the Programa Estatal de Fomento de la Investigación Científica y Técnica de Excelencia María de Maeztu, Grant MDM-2015-0509 and the Programa Severo Ochoa del Principado de Asturias; the Thalis and Aristeia programs cofinanced by EU-ESF and the Greek NSRF; the Rachadapisek Sompot Fund for Postdoctoral Fellowship, Chulalongkorn University and the Chulalongkorn Academic into Its 2nd Century Project Advancement Project (Thailand); the Welch Foundation, contract C-1845; and the Weston Havens Foundation (USA).

Data Availability Statement This manuscript has no associated data or the data will not be deposited [Authors' comment: Release and preservation of data used by the CMS Collaboration as the basis for publications is guided by the CMS policy as written in its document "CMS data preservation, re-use and open access policy" (https://cms-docb.cern.ch/cgi-bin/PublicDocDB/RetrieveFile?docid=6032&filename=CMSDataPolicyV1.2.pdf&version=2).]

Funded by SCOAP[3].

References

1. F. Zwicky, Die Rotverschiebung von extragalaktischen Nebeln. Helv. Phys. Acta **6**, 110 (1933)
2. V.C. Rubin, W.K. Ford Jr., Rotation of the Andromeda nebula from a spectroscopic survey of emission regions. Astrophys. J. **159**, 379 (1970). https://doi.org/10.1086/150317
3. R. Barbieri, G.F. Giudice, Upper bounds on supersymmetric particle masses. Nucl. Phys. B **306**, 63 (1988). https://doi.org/10.1016/0550-3213(88)90171-X
4. S. Dimopoulos, G.F. Giudice, Naturalness constraints in supersymmetric theories with nonuniversal soft terms. Phys. Lett. B **357**, 573 (1995). https://doi.org/10.1016/0370-2693(95)00961-J. arXiv:hep-ph/9507282
5. R. Barbieri, D. Pappadopulo, S-particles at their naturalness limits. JHEP **10**, 061 (2009). https://doi.org/10.1088/1126-6708/2009/10/061. arXiv:0906.4546
6. M. Papucci, J.T. Ruderman, A. Weiler, Natural SUSY endures. JHEP **09**, 035 (2012). https://doi.org/10.1007/JHEP09(2012)035. arXiv:1110.6926
7. CMS Collaboration, Measurements of properties of the Higgs boson decaying into the four-lepton final state in pp collisions at $\sqrt{s} = 13$ TeV. JHEP **11**, 047 (2017). https://doi.org/10.1007/JHEP11(2017)047. arXiv:1706.09936
8. ATLAS and CMS Collaborations, Combined measurement of the Higgs boson mass in pp collisions at $\sqrt{s} = 7$ and 8 TeV with the ATLAS and CMS experiments. Phys. Rev. Lett. **114**, 191803 (2015). https://doi.org/10.1103/PhysRevLett.114.191803. arXiv:1503.07589
9. P. Ramond, Dual theory for free fermions. Phys. Rev. D **3**, 2415 (1971). https://doi.org/10.1103/PhysRevD.3.2415
10. YuA Golfand, E.P. Likhtman, Extension of the algebra of Poincaré group generators and violation of P invariance. JETP Lett. **13**, 323 (1971)
11. A. Neveu, J.H. Schwarz, Factorizable dual model of pions. Nucl. Phys. B **31**, 86 (1971). https://doi.org/10.1016/0550-3213(71)90448-2
12. D.V. Volkov, V.P. Akulov, Possible universal neutrino interaction. JETP Lett. **16**, 438 (1972)
13. J. Wess, B. Zumino, A Lagrangian model invariant under supergauge transformations. Phys. Lett. B **49**, 52 (1974). https://doi.org/10.1016/0370-2693(74)90578-4
14. J. Wess, B. Zumino, Supergauge transformations in four dimensions. Nucl. Phys. B **70**, 39 (1974). https://doi.org/10.1016/0550-3213(74)90355-1
15. P. Fayet, Supergauge invariant extension of the Higgs mechanism and a model for the electron and its neutrino. Nucl. Phys. B **90**, 104 (1975). https://doi.org/10.1016/0550-3213(75)90636-7
16. H.P. Nilles, Supersymmetry, supergravity and particle physics. Phys. Rep. **110**, 1 (1984). https://doi.org/10.1016/0370-1573(84)90008-5
17. G.R. Farrar, P. Fayet, Phenomenology of the production, decay, and detection of new hadronic states associated with supersymmetry. Phys. Lett. B **76**, 575 (1978). https://doi.org/10.1016/0370-2693(78)90858-4
18. P. Meade, N. Seiberg, D. Shih, General gauge mediation. Prog. Theor. Phys. Suppl. **177**, 143 (2009). https://doi.org/10.1143/PTPS.177.143. arXiv:0801.3278
19. S. Deser, B. Zumino, Broken supersymmetry and supergravity. Phys. Rev. Lett. **38**, 1433 (1977). https://doi.org/10.1103/PhysRevLett.38.1433
20. E. Cremmer et al., Super-Higgs effect in supergravity with general scalar interactions. Phys. Lett. B **79**, 231 (1978). https://doi.org/10.1016/0370-2693(78)90230-7
21. N. Arkani-Hamed et al., MARMOSET: the path from LHC data to the new standard model via on-shell effective theories. (2007). arXiv:hep-ph/0703088
22. J. Alwall, P.C. Schuster, N. Toro, Simplified models for a first characterization of new physics at the LHC. Phys. Rev. D **79**, 075020 (2009). https://doi.org/10.1103/PhysRevD.79.075020. arXiv:0810.3921
23. J. Alwall, M.-P. Le, M. Lisanti, J.G. Wacker, Model-independent jets plus missing energy searches. Phys. Rev. D **79**, 015005 (2009). https://doi.org/10.1103/PhysRevD.79.015005. arXiv:0809.3264
24. D. Alves et al., Simplified models for LHC new physics searches. J. Phys. G **39**, 105005 (2012). https://doi.org/10.1088/0954-3899/39/10/105005. arXiv:1105.2838
25. CMS Collaboration, Interpretation of searches for supersymmetry with simplified models. Phys. Rev. D **88**, 052017 (2013). https://doi.org/10.1103/PhysRevD.88.052017. arXiv:1301.2175
26. CMS Collaboration, CMS luminosity measurements for the 2016 data taking period. CMS Physics Analysis Summary CMS-PAS-LUM-17-001 (2017)
27. CMS Collaboration, Search for gauge-mediated supersymmetry in events with at least one photon and missing transverse momentum in pp collisions at $\sqrt{s} = 13$ TeV. Phys. Lett. B **780**, 118 (2018). https://doi.org/10.1016/j.physletb.2018.02.045. arXiv:1711.08008
28. CMS Collaboration, Search for supersymmetry in events with at least one photon, missing transverse momentum, and large transverse event activity in proton–proton collisions at $\sqrt{s} = 13$ TeV. JHEP **12**, 142 (2017). https://doi.org/10.1007/JHEP12(2017)142. arXiv:1707.06193
29. ATLAS Collaboration, Search for photonic signatures of gauge-mediated supersymmetry in 8 TeV pp collisions with the ATLAS detector. Phys. Rev. D **92**, 072001 (2015). https://doi.org/10.1103/PhysRevD.92.072001. arXiv:1507.05493

30. ATLAS Collaboration, Search for supersymmetry in a final state containing two photons and missing transverse momentum in $\sqrt{s}$ = 13 TeV pp collisions at the LHC using the ATLAS detector. Eur. Phys. J. C **76**, 517 (2016). https://doi.org/10.1140/epjc/s10052-016-4344-x. arXiv:1606.09150
31. ATLAS Collaboration, Search for photonic signatures of gauge-mediated supersymmetry in 13 TeV pp collisions with the ATLAS detector. Phys. Rev. D **97**, 092006 (2018). https://doi.org/10.1103/PhysRevD.97.092006. arXiv:1802.03158
32. CMS Collaboration, The CMS experiment at the CERN LHC. JINST **3**, S08004 (2008). https://doi.org/10.1088/1748-0221/3/08/S08004
33. CMS Collaboration, The CMS trigger system. JINST **12**, P01020 (2017). https://doi.org/10.1088/1748-0221/12/01/P01020. arXiv:1609.02366
34. J. Alwall et al., The automated computation of tree-level and next-to-leading order differential cross sections, and their matching to parton shower simulations. JHEP **07**, 079 (2014). https://doi.org/10.1007/JHEP07(2014)079. arXiv:1405.0301
35. A. Kalogeropoulos, J. Alwall, The SysCalc code: A tool to derive theoretical systematic uncertainties, (2018). arXiv:1801.08401
36. P. Artoisenet, R. Frederix, O. Mattelaer, R. Rietkerk, Automatic spin-entangled decays of heavy resonances in Monte Carlo simulations. JHEP **03**, 015 (2013). https://doi.org/10.1007/JHEP03(2013)015. arXiv:1212.3460
37. M. Czakon, A. Mitov, Top++: A program for the calculation of the top-pair cross-section at hadron colliders. Comput. Phys. Commun. **185**, 2930 (2014). https://doi.org/10.1016/j.cpc.2014.06.021. arXiv:1112.5675
38. R. Gavin, Y. Li, F. Petriello, S. Quackenbush, W physics at the LHC with FEWZ 2.1. Comput. Phys. Commun **184**, 208 (2013). https://doi.org/10.1016/j.cpc.2012.09.005. arXiv:1201.5896
39. R. Gavin, Y. Li, F. Petriello, S. Quackenbush, FEWZ 2.0: a code for hadronic Z production at next-to-next-to-leading order. Comput. Phys. Commun **182**, 2388 (2011). https://doi.org/10.1016/j.cpc.2011.06.008. arXiv:1011.3540
40. NNPDF Collaboration, Parton distributions for the LHC Run II. JHEP **04**, 040 (2015). https://doi.org/10.1007/JHEP04(2015)040. arXiv:1410.8849
41. T. Sjöstrand et al., An introduction to PYTHIA 8.2. Comput. Phys. Commun **191**, 159 (2015). https://doi.org/10.1016/j.cpc.2015.01.024. arXiv:1410.3012
42. CMS Collaboration, Event generator tunes obtained from underlying event and multiparton scattering measurements. Eur. Phys. J. C **76**, 155 (2016). https://doi.org/10.1140/epjc/s10052-016-3988-x. arXiv:1512.00815
43. J. Alwall et al., Comparative study of various algorithms for the merging of parton showers and matrix elements in hadronic collisions. Eur. Phys. J. C **53**, 473 (2008). https://doi.org/10.1140/epjc/s10052-007-0490-5. arXiv:0706.2569
44. R. Frederix, S. Frixione, Merging meets matching in MC@NLO. JHEP **12**, 061 (2012). https://doi.org/10.1007/JHEP12(2012)061. arXiv:1209.6215
45. W. Beenakker, R. Höpker, M. Spira, P.M. Zerwas, Squark and gluino production at hadron colliders. Nucl. Phys. B **492**, 51 (1997). https://doi.org/10.1016/S0550-3213(97)00084-9. arXiv:hep-ph/9610490
46. A. Kulesza, L. Motyka, Threshold resummation for squark-antisquark and gluino-pair production at the LHC. Phys. Rev. Lett. **102**, 111802 (2009). https://doi.org/10.1103/PhysRevLett.102.111802. arXiv:0807.2405
47. A. Kulesza, L. Motyka, Soft gluon resummation for the production of gluino-gluino and squark-antisquark pairs at the LHC. Phys. Rev. D **80**, 095004 (2009). https://doi.org/10.1103/PhysRevD.80.095004. arXiv:0905.4749
48. W. Beenakker et al., Soft-gluon resummation for squark and gluino hadroproduction. JHEP **12**, 041 (2009). https://doi.org/10.1088/1126-6708/2009/12/041. arXiv:0909.4418
49. W. Beenakker et al., Squark and gluino hadroproduction. Int. J. Mod. Phys. A **26**, 2637 (2011). https://doi.org/10.1142/S0217751X11053560. arXiv:1105.1110
50. GEANT4 Collaboration, Geant4–a simulation toolkit. Nucl. Instrum. Meth. A **506**, 250 (2003). https://doi.org/10.1016/S0168-9002(03)01368-8
51. S. Abdullin et al., The fast simulation of the CMS detector at LHC. J. Phys. Conf. Ser. **331**, 032049 (2011). https://doi.org/10.1088/1742-6596/331/3/032049
52. A. Giammanco, The fast simulation of the CMS experiment. J. Phys. Conf. Ser. **513**, 022012 (2014). https://doi.org/10.1088/1742-6596/513/2/022012
53. CMS Collaboration, Particle-flow reconstruction and global event description with the CMS detector. JINST **12**, P10003 (2017). https://doi.org/10.1088/1748-0221/12/10/P10003. arXiv:1706.04965
54. C.M.S. Collaboration, Performance of electron reconstruction and selection with the CMS detector in proton–proton collisions at $\sqrt{s}$ = 8 TeV. JINST **10**, P06005 (2015). https://doi.org/10.1088/1748-0221/10/06/P06005. arXiv:1502.02701
55. CMS Collaboration, Performance of photon reconstruction and identification with the CMS detector in proton–proton collisions at $\sqrt{s}$ = 8 TeV. JINST **10**, P08010 (2015). https://doi.org/10.1088/1748-0221/10/08/P08010. arXiv:1502.02702
56. C.M.S. Collaboration, Performance of the CMS muon detector and muon reconstruction with proton–proton collisions at $\sqrt{s}$ = 13 TeV. JINST **13**, P06015 (2018). https://doi.org/10.1088/1748-0221/13/06/P06015. arXiv:1804.04528
57. M. Cacciari, G.P. Salam, G. Soyez, The anti-k_{T} jet clustering algorithm. JHEP **04**, 063 (2008). https://doi.org/10.1088/1126-6708/2008/04/063. arXiv:0802.1189
58. M. Cacciari, G.P. Salam, G. Soyez, FastJet user manual. Eur. Phys. J. C **72**, 1896 (2012). https://doi.org/10.1140/epjc/s10052-012-1896-2. arXiv:1111.6097
59. CMS Collaboration, Jet algorithms performance in 13 TeV data. CMS Physics Analysis Summary CMS-PAS-JME-16-003 (2017)
60. C.M.S. Collaboration, Jet energy scale and resolution in the CMS experiment in pp collisions at 8 TeV. JINST **12**, P02014 (2017). https://doi.org/10.1088/1748-0221/12/02/P02014. arXiv:1607.03663
61. M. Cacciari, G.P. Salam, Pileup subtraction using jet areas. Phys. Lett. B **659**, 119 (2008). https://doi.org/10.1016/j.physletb.2007.09.077. arXiv:0707.1378
62. CMS Collaboration, Identification of heavy-flavour jets with the CMS detector in pp collisions at 13 TeV. JINST **13**, P05011 (2018). https://doi.org/10.1088/1748-0221/13/05/P05011. arXiv:1712.07158
63. K. Rehermann, B. Tweedie, Efficient identification of boosted semileptonic top quarks at the LHC. JHEP **03**, 059 (2011). https://doi.org/10.1007/JHEP03(2011)059. arXiv:1007.2221
64. CMS Collaboration, Performance of missing energy reconstruction in 13 TeV pp collision data using the CMS detector. CMS Physics Analysis Summary CMS-PAS-JME-16-004 (2016)
65. M. Cacciari et al., The $t\bar{t}$ cross-section at 1.8 TeV and 1.96 TeV: a study of the systematics due to parton densities and scale dependence. JHEP **04**, 068 (2004). https://doi.org/10.1088/1126-6708/2004/04/068. arXiv:hep-ph/0303085
66. S. Catani, D. de Florian, M. Grazzini, P. Nason, Soft gluon resummation for Higgs boson production at hadron colliders. JHEP **07**, 028 (2003). https://doi.org/10.1088/1126-6708/2003/07/028. arXiv:hep-ph/0306211
67. A. Denner, S. Dittmaier, M. Hecht, C. Pasold, NLO QCD and electroweak corrections to $Z + \gamma$ production with leptonic Z-

69. G. Cowan, K. Cranmer, E. Gross, O. Vitells, Asymptotic formulae for likelihood-based tests of new physics. Eur. Phys. J. C **71**, 1554 (2011). https://doi.org/10.1140/epjc/s10052-011-1554-0. arXiv:1007.1727. [Erratum: 10.1140/epjc/s10052-013-2501-z]
70. T. Junk, Confidence level computation for combining searches with small statistics. Nucl. Instrum. Meth. A **434**, 435 (1999). https://doi.org/10.1016/S0168-9002(99)00498-2. arXiv:hep-ex/9902006
71. A.L. Read, Presentation of search results: the CL_s technique. J. Phys. G **28**, 2693 (2002). https://doi.org/10.1088/0954-3899/28/10/313

CMS Collaboration

Yerevan Physics Institute, Yerevan, Armenia
A. M. Sirunyan, A. Tumasyan

Institut für Hochenergiephysik, Wien, Austria
W. Adam, F. Ambrogi, E. Asilar, T. Bergauer, J. Brandstetter, M. Dragicevic, J. Erö, A. Escalante Del Valle, M. Flechl, R. Frühwirth[1], V. M. Ghete, J. Hrubec, M. Jeitler[1], N. Krammer, I. Krätschmer, D. Liko, T. Madlener, I. Mikulec, N. Rad, H. Rohringer, J. Schieck[1], R. Schöfbeck, M. Spanring, D. Spitzbart, W. Waltenberger, J. Wittmann, C.-E. Wulz[1], M. Zarucki

Institute for Nuclear Problems, Minsk, Belarus
V. Chekhovsky, V. Mossolov, J. Suarez Gonzalez

Universiteit Antwerpen, Antwerpen, Belgium
E. A. De Wolf, D. Di Croce, X. Janssen, J. Lauwers, M. Pieters, H. Van Haevermaet, P. Van Mechelen, N. Van Remortel

Vrije Universiteit Brussel, Brussels, Belgium
S. Abu Zeid, F. Blekman, J. D'Hondt, J. De Clercq, K. Deroover, G. Flouris, D. Lontkovskyi, S. Lowette, I. Marchesini, S. Moortgat, L. Moreels, Q. Python, K. Skovpen, S. Tavernier, W. Van Doninck, P. Van Mulders, I. Van Parijs

Université Libre de Bruxelles, Brussels, Belgium
D. Beghin, B. Bilin, H. Brun, B. Clerbaux, G. De Lentdecker, H. Delannoy, B. Dorney, G. Fasanella, L. Favart, R. Goldouzian, A. Grebenyuk, A. K. Kalsi, T. Lenzi, J. Luetic, N. Postiau, E. Starling, L. Thomas, C. Vander Velde, P. Vanlaer, D. Vannerom, Q. Wang

Ghent University, Ghent, Belgium
T. Cornelis, D. Dobur, A. Fagot, M. Gul, I. Khvastunov[2], D. Poyraz, C. Roskas, D. Trocino, M. Tytgat, W. Verbeke, B. Vermassen, M. Vit, N. Zaganidis

Université Catholique de Louvain, Louvain-la-Neuve, Belgium
H. Bakhshiansohi, O. Bondu, S. Brochet, G. Bruno, C. Caputo, P. David, C. Delaere, M. Delcourt, A. Giammanco, G. Krintiras, V. Lemaitre, A. Magitteri, K. Piotrzkowski, A. Saggio, M. Vidal Marono, P. Vischia, S. Wertz, J. Zobec

Centro Brasileiro de Pesquisas Fisicas, Rio de Janeiro, Brazil
F. L. Alves, G. A. Alves, G. Correia Silva, C. Hensel, A. Moraes, M. E. Pol, P. Rebello Teles

Universidade do Estado do Rio de Janeiro, Rio de Janeiro, Brazil
E. Belchior Batista Das Chagas, W. Carvalho, J. Chinellato[3], E. Coelho, E. M. Da Costa, G. G. Da Silveira[4], D. De Jesus Damiao, C. De Oliveira Martins, S. Fonseca De Souza, H. Malbouisson, D. Matos Figueiredo, M. Melo De Almeida, C. Mora Herrera, L. Mundim, H. Nogima, W. L. Prado Da Silva, L. J. Sanchez Rosas, A. Santoro, A. Sznajder, M. Thiel, E. J. Tonelli Manganote[3], F. Torres Da Silva De Araujo, A. Vilela Pereira

Universidade Estadual Paulista [a], Universidade Federal do ABC [b], São Paulo, Brazil
S. Ahuja[a], C. A. Bernardes[a], L. Calligaris[a], T. R. Fernandez Perez Tomei[a], E. M. Gregores[b], P. G. Mercadante[b], S. F. Novaes[a], SandraS. Padula[a]

Institute for Nuclear Research and Nuclear Energy, Bulgarian Academy of Sciences, Sofia, Bulgaria
A. Aleksandrov, R. Hadjiiska, P. Iaydjiev, A. Marinov, M. Misheva, M. Rodozov, M. Shopova, G. Sultanov

University of Sofia, Sofia, Bulgaria
A. Dimitrov, L. Litov, B. Pavlov, P. Petkov

Beihang University, Beijing, China
W. Fang[5], X. Gao[5], L. Yuan

Institute of High Energy Physics, Beijing, China
M. Ahmad, J. G. Bian, G. M. Chen, H. S. Chen, M. Chen, Y. Chen, C. H. Jiang, D. Leggat, H. Liao, Z. Liu, S. M. Shaheen[6], A. Spiezia, J. Tao, E. Yazgan, H. Zhang, S. Zhang[6], J. Zhao

State Key Laboratory of Nuclear Physics and Technology, Peking University, Beijing, China
Y. Ban, G. Chen, A. Levin, J. Li, L. Li, Q. Li, Y. Mao, S. J. Qian, D. Wang

Tsinghua University, Beijing, China
Y. Wang

Universidad de Los Andes, Bogota, Colombia
C. Avila, A. Cabrera, C. A. Carrillo Montoya, L. F. Chaparro Sierra, C. Florez, C. F. González Hernández, M. A. Segura Delgado

University of Split, Faculty of Electrical Engineering, Mechanical Engineering and Naval Architecture, Split, Croatia
B. Courbon, N. Godinovic, D. Lelas, I. Puljak, T. Sculac

University of Split, Faculty of Science, Split, Croatia
Z. Antunovic, M. Kovac

Institute Rudjer Boskovic, Zagreb, Croatia
V. Brigljevic, D. Ferencek, K. Kadija, B. Mesic, M. Roguljic, A. Starodumov[7], T. Susa

University of Cyprus, Nicosia, Cyprus
M. W. Ather, A. Attikis, M. Kolosova, G. Mavromanolakis, J. Mousa, C. Nicolaou, F. Ptochos, P. A. Razis, H. Rykaczewski

Charles University, Prague, Czech Republic
M. Finger[8], M. Finger Jr.[8]

Escuela Politecnica Nacional, Quito, Ecuador
E. Ayala

Universidad San Francisco de Quito, Quito, Ecuador
E. Carrera Jarrin

Academy of Scientific Research and Technology of the Arab Republic of Egypt, Egyptian Network of High Energy Physics, Cairo, Egypt
A. Ellithi Kamel[9], S. Khalil[10], E. Salama[11,12]

National Institute of Chemical Physics and Biophysics, Tallinn, Estonia
S. Bhowmik, A. Carvalho Antunes De Oliveira, R. K. Dewanjee, K. Ehataht, M. Kadastik, M. Raidal, C. Veelken

Department of Physics, University of Helsinki, Helsinki, Finland
P. Eerola, H. Kirschenmann, J. Pekkanen, M. Voutilainen

Helsinki Institute of Physics, Helsinki, Finland
J. Havukainen, J. K. Heikkilä, T. Järvinen, V. Karimäki, R. Kinnunen, T. Lampén, K. Lassila-Perini, S. Laurila, S. Lehti, T. Lindén, P. Luukka, T. Mäenpää, H. Siikonen, E. Tuominen, J. Tuominiemi

Lappeenranta University of Technology, Lappeenranta, Finland
T. Tuuva

IRFU, CEA, Université Paris-Saclay, Gif-sur-Yvette, France
M. Besancon, F. Couderc, M. Dejardin, D. Denegri, J. L. Faure, F. Ferri, S. Ganjour, A. Givernaud, P. Gras, G. Hamel de Monchenault, P. Jarry, C. Leloup, E. Locci, J. Malcles, G. Negro, J. Rander, A. Rosowsky, M. Ö. Sahin, M. Titov

Laboratoire Leprince-Ringuet, Ecole polytechnique, CNRS/IN2P3, Université Paris-Saclay, Palaiseau, France
A. Abdulsalam[13], C. Amendola, I. Antropov, F. Beaudette, P. Busson, C. Charlot, R. Granier de Cassagnac, I. Kucher,

A. Lobanov, J. Martin Blanco, C. Martin Perez, M. Nguyen, C. Ochando, G. Ortona, P. Paganini, J. Rembser, R. Salerno, J. B. Sauvan, Y. Sirois, A. G. Stahl Leiton, A. Zabi, A. Zghiche

Université de Strasbourg, CNRS, IPHC UMR 7178, Strasbourg, France
J.-L. Agram[14], J. Andrea, D. Bloch, J.-M. Brom, E. C. Chabert, V. Cherepanov, C. Collard, E. Conte[14], J.-C. Fontaine[14], D. Gelé, U. Goerlach, M. Jansová, A.-C. Le Bihan, N. Tonon, P. Van Hove

Centre de Calcul de l'Institut National de Physique Nucleaire et de Physique des Particules, CNRS/IN2P3, Villeurbanne, France
S. Gadrat

Université de Lyon, Université Claude Bernard Lyon 1, CNRS-IN2P3, Institut de Physique Nucléaire de Lyon, Villeurbanne, France
S. Beauceron, C. Bernet, G. Boudoul, N. Chanon, R. Chierici, D. Contardo, P. Depasse, H. El Mamouni, J. Fay, L. Finco, S. Gascon, M. Gouzevitch, G. Grenier, B. Ille, F. Lagarde, I. B. Laktineh, H. Lattaud, M. Lethuillier, L. Mirabito, S. Perries, A. Popov[15], V. Sordini, G. Touquet, M. Vander Donckt, S. Viret

Georgian Technical University, Tbilisi, Georgia
T. Toriashvili[16]

Tbilisi State University, Tbilisi, Georgia
Z. Tsamalaidze[8]

RWTH Aachen University, I. Physikalisches Institut, Aachen, Germany
C. Autermann, L. Feld, M. K. Kiesel, K. Klein, M. Lipinski, M. Preuten, M. P. Rauch, C. Schomakers, J. Schulz, M. Teroerde, B. Wittmer

RWTH Aachen University, III. Physikalisches Institut A, Aachen, Germany
A. Albert, D. Duchardt, M. Erdmann, S. Erdweg, T. Esch, R. Fischer, S. Ghosh, A. Güth, T. Hebbeker, C. Heidemann, K. Hoepfner, H. Keller, L. Mastrolorenzo, M. Merschmeyer, A. Meyer, P. Millet, S. Mukherjee, T. Pook, M. Radziej, H. Reithler, M. Rieger, A. Schmidt, D. Teyssier, S. Thüer

RWTH Aachen University, III. Physikalisches Institut B, Aachen, Germany
G. Flügge, O. Hlushchenko, T. Kress, T. Müller, A. Nehrkorn, A. Nowack, C. Pistone, O. Pooth, D. Roy, H. Sert, A. Stahl[17]

Deutsches Elektronen-Synchrotron, Hamburg, Germany
M. Aldaya Martin, T. Arndt, C. Asawatangtrakuldee, I. Babounikau, K. Beernaert, O. Behnke, U. Behrens, A. Bermúdez Martínez, D. Bertsche, A. A. Bin Anuar, K. Borras[18], V. Botta, A. Campbell, P. Connor, C. Contreras-Campana, V. Danilov, A. De Wit, M. M. Defranchis, C. Diez Pardos, D. Domínguez Damiani, G. Eckerlin, T. Eichhorn, A. Elwood, E. Eren, E. Gallo[19], A. Geiser, J. M. Grados Luyando, A. Grohsjean, M. Guthoff, M. Haranko, A. Harb, H. Jung, M. Kasemann, J. Keaveney, C. Kleinwort, J. Knolle, D. Krücker, W. Lange, A. Lelek, T. Lenz, J. Leonard, K. Lipka, W. Lohmann[20], R. Mankel, I.-A. Melzer-Pellmann, A. B. Meyer, M. Meyer, M. Missiroli, G. Mittag, J. Mnich, V. Myronenko, S. K. Pflitsch, D. Pitzl, A. Raspereza, M. Savitskyi, P. Saxena, P. Schütze, C. Schwanenberger, R. Shevchenko, A. Singh, H. Tholen, O. Turkot, A. Vagnerini, M. Van De Klundert, G. P. Van Onsem, R. Walsh, Y. Wen, K. Wichmann, C. Wissing, O. Zenaiev

University of Hamburg, Hamburg, Germany
R. Aggleton, S. Bein, L. Benato, A. Benecke, T. Dreyer, A. Ebrahimi, E. Garutti, D. Gonzalez, P. Gunnellini, J. Haller, A. Hinzmann, A. Karavdina, G. Kasieczka, R. Klanner, R. Kogler, N. Kovalchuk, S. Kurz, V. Kutzner, J. Lange, D. Marconi, J. Multhaup, M. Niedziela, C.E.N. Niemeyer, D. Nowatschin, A. Perieanu, A. Reimers, O. Rieger, C. Scharf, P. Schleper, S. Schumann, J. Schwandt, J. Sonneveld, H. Stadie, G. Steinbrück, F. M. Stober, M. Stöver, B. Vormwald, I. Zoi

Karlsruher Institut fuer Technologie, Karlsruhe, Germany
M. Akbiyik, C. Barth, M. Baselga, S. Baur, E. Butz, R. Caspart, T. Chwalek, F. Colombo, W. De Boer, A. Dierlamm, K. El Morabit, N. Faltermann, B. Freund, M. Giffels, M. A. Harrendorf, F. Hartmann[17], S. M. Heindl, U. Husemann, I. Katkov[15], S. Kudella, S. Mitra, M. U. Mozer, Th. Müller, M. Musich, M. Plagge, G. Quast, K. Rabbertz, M. Schröder, I. Shvetsov, H. J. Simonis, R. Ulrich, S. Wayand, M. Weber, T. Weiler, C. Wöhrmann, R. Wolf

Institute of Nuclear and Particle Physics (INPP), NCSR Demokritos, Aghia Paraskevi, Greece
G. Anagnostou, G. Daskalakis, T. Geralis, A. Kyriakis, D. Loukas, G. Paspalaki

National and Kapodistrian University of Athens, Athens, Greece
A. Agapitos, G. Karathanasis, P. Kontaxakis, A. Panagiotou, I. Papavergou, N. Saoulidou, E. Tziaferi, K. Vellidis

National Technical University of Athens, Athens, Greece
K. Kousouris, I. Papakrivopoulos, G. Tsipolitis

University of Ioánnina, Ioánnina, Greece
I. Evangelou, C. Foudas, P. Gianneios, P. Katsoulis, P. Kokkas, S. Mallios, N. Manthos, I. Papadopoulos, E. Paradas, J. Strologas, F. A. Triantis, D. Tsitsonis

MTA-ELTE Lendület CMS Particle and Nuclear Physics Group, Eötvös Loránd University, Budapest, Hungary
M. Bartók[21], M. Csanad, N. Filipovic, P. Major, M. I. Nagy, G. Pasztor, O. Surányi, G. I. Veres

Wigner Research Centre for Physics, Budapest, Hungary
G. Bencze, C. Hajdu, D. Horvath[22], Á. Hunyadi, F. Sikler, T. Á. Vámi, V. Veszpremi, G. Vesztergombi[†]

Institute of Nuclear Research ATOMKI, Debrecen, Hungary
N. Beni, S. Czellar, J. Karancsi[21], A. Makovec, J. Molnar, Z. Szillasi

Institute of Physics, University of Debrecen, Debrecen, Hungary
P. Raics, Z. L. Trocsanyi, B. Ujvari

Indian Institute of Science (IISc), Bangalore, India
S. Choudhury, J. R. Komaragiri, P. C. Tiwari

National Institute of Science Education and Research, HBNI, Bhubaneswar, India
S. Bahinipati[24], C. Kar, P. Mal, K. Mandal, A. Nayak[25], S. Roy Chowdhury, D. K. Sahoo[24], S. K. Swain

Panjab University, Chandigarh, India
S. Bansal, S. B. Beri, V. Bhatnagar, S. Chauhan, R. Chawla, N. Dhingra, R. Gupta, A. Kaur, M. Kaur, S. Kaur, P. Kumari, M. Lohan, M. Meena, A. Mehta, K. Sandeep, S. Sharma, J. B. Singh, A. K. Virdi, G. Walia

University of Delhi, Delhi, India
A. Bhardwaj, B. C. Choudhary, R. B. Garg, M. Gola, S. Keshri, Ashok Kumar, S. Malhotra, M. Naimuddin, P. Priyanka, K. Ranjan, Aashaq Shah, R. Sharma

Saha Institute of Nuclear Physics, HBNI, Kolkata, India
R. Bhardwaj[26], M. Bharti[26], R. Bhattacharya, S. Bhattacharya, U. Bhawandeep[26], D. Bhowmik, S. Dey, S. Dutt[26], S. Dutta, S. Ghosh, M. Maity[27], K. Mondal, S. Nandan, A. Purohit, P. K. Rout, A. Roy, G. Saha, S. Sarkar, T. Sarkar[27], M. Sharan, B. Singh[26], S. Thakur[26]

Indian Institute of Technology Madras, Madras, India
P. K. Behera, A. Muhammad

Bhabha Atomic Research Centre, Mumbai, India
R. Chudasama, D. Dutta, V. Jha, V. Kumar, D. K. Mishra, P. K. Netrakanti, L. M. Pant, P. Shukla, P. Suggisetti

Tata Institute of Fundamental Research-A, Mumbai, India
T. Aziz, M. A. Bhat, S. Dugad, G. B. Mohanty, N. Sur, RavindraKumar Verma

Tata Institute of Fundamental Research-B, Mumbai, India
S. Banerjee, S. Bhattacharya, S. Chatterjee, P. Das, M. Guchait, Sa. Jain, S. Karmakar, S. Kumar, G. Majumder, K. Mazumdar, N. Sahoo

Indian Institute of Science Education and Research (IISER), Pune, India
S. Chauhan, S. Dube, V. Hegde, A. Kapoor, K. Kothekar, S. Pandey, A. Rane, A. Rastogi, S. Sharma

Institute for Research in Fundamental Sciences (IPM), Tehran, Iran
S. Chenarani[28], E. Eskandari Tadavani, S. M. Etesami[28], M. Khakzad, M. Mohammadi Najafabadi, M. Naseri, F. Rezaei Hosseinabadi, B. Safarzadeh[29], M. Zeinali

University College Dublin, Dublin, Ireland
M. Felcini, M. Grunewald

INFN Sezione di Bari[a], Università di Bari[b], Politecnico di Bari[c], Bari, Italy
M. Abbrescia[a,b], C. Calabria[a,b], A. Colaleo[a], D. Creanza[a,c], L. Cristella[a,b], N. De Filippis[a,c], M. De Palma[a,b], A. Di Florio[a,b], F. Errico[a,b], L. Fiore[a], A. Gelmi[a,b], G. Iaselli[a,c], M. Ince[a,b], S. Lezki[a,b], G. Maggi[a,c], M. Maggi[a], G. Miniello[a,b], S. My[a,b], S. Nuzzo[a,b], A. Pompili[a,b], G. Pugliese[a,c], R. Radogna[a], A. Ranieri[a], G. Selvaggi[a,b], A. Sharma[a], L. Silvestris[a], R. Venditti[a], P. Verwilligen[a]

INFN Sezione di Bologna[a], Università di Bologna[b], Bologna, Italy
G. Abbiendi[a], C. Battilana[a,b], D. Bonacorsi[a,b], L. Borgonovi[a,b], S. Braibant-Giacomelli[a,b], R. Campanini[a,b], P. Capiluppi[a,b], A. Castro[a,b], F. R. Cavallo[a], S. S. Chhibra[a,b], G. Codispoti[a,b], M. Cuffiani[a,b], G. M. Dallavalle[a], F. Fabbri[a], A. Fanfani[a,b], E. Fontanesi, P. Giacomelli[a], C. Grandi[a], L. Guiducci[a,b], F. Iemmi[a,b], S. Lo Meo[a,30], S. Marcellini[a], G. Masetti[a], A. Montanari[a], F. L. Navarria[a,b], A. Perrotta[a], F. Primavera[a,b], A. M. Rossi[a,b], T. Rovelli[a,b], G. P. Siroli[a,b], N. Tosi[a]

INFN Sezione di Catania[a], Università di Catania[b], Catania, Italy
S. Albergo[a,b], A. Di Mattia[a], R. Potenza[a,b], A. Tricomi[a,b], C. Tuve[a,b]

INFN Sezione di Firenze[a], Università di Firenze[b], Florence, Italy
G. Barbagli[a], K. Chatterjee[a,b], V. Ciulli[a,b], C. Civinini[a], R. D'Alessandro[a,b], E. Focardi[a,b], G. Latino, P. Lenzi[a,b], M. Meschini[a], S. Paoletti[a], L. Russo[a,31], G. Sguazzoni[a], D. Strom[a], L. Viliani[a]

INFN Laboratori Nazionali di Frascati, Frascati, Italy
L. Benussi, S. Bianco, F. Fabbri, D. Piccolo

INFN Sezione di Genova[a], Università di Genova[b], Genoa, Italy
F. Ferro[a], R. Mulargia[a,b], E. Robutti[a], S. Tosi[a,b]

INFN Sezione di Milano-Bicocca[a], Università di Milano-Bicocca[b], Milan, Italy
A. Benaglia[a], A. Beschi[b], F. Brivio[a,b], V. Ciriolo[a,b,17], S. Di Guida[a,b,17], M. E. Dinardo[a,b], S. Fiorendi[a,b], S. Gennai[a], A. Ghezzi[a,b], P. Govoni[a,b], M. Malberti[a,b], S. Malvezzi[a], D. Menasce[a], F. Monti, L. Moroni[a], M. Paganoni[a,b], D. Pedrini[a], S. Ragazzi[a,b], T. Tabarelli de Fatis[a,b], D. Zuolo[a,b]

INFN Sezione di Napoli[a], Università di Napoli 'Federico II' [b], Napoli, Italy, Università della Basilicata[c], Potenza, Italy, Università G. Marconi[d], Rome, Italy
S. Buontempo[a], N. Cavallo[a,c], A. De Iorio[a,b], A. Di Crescenzo[a,b], F. Fabozzi[a,c], F. Fienga[a], G. Galati[a], A. O. M. Iorio[a,b], L. Lista[a], S. Meola[a,d,17], P. Paolucci[a,17], C. Sciacca[a,b], E. Voevodina[a,b]

INFN Sezione di Padova[a], Università di Padova[b], Padova, Italy, Università di Trento[c], Trento, Italy
P. Azzi[a], N. Bacchetta[a], D. Bisello[a,b], A. Boletti[a,b], A. Bragagnolo, R. Carlin[a,b], P. Checchia[a], M. Dall'Osso[a,b], P. De Castro Manzano[a], T. Dorigo[a], U. Dosselli[a], F. Gasparini[a,b], U. Gasparini[a,b], A. Gozzelino[a], S. Y. Hoh, S. Lacaprara[a], P. Lujan, M. Margoni[a,b], A. T. Meneguzzo[a,b], J. Pazzini[a,b], M. Presilla[b], P. Ronchese[a,b], R. Rossin[a,b], F. Simonetto[a,b], A. Tiko, E. Torassa[a], M. Tosi[a,b], M. Zanetti[a,b], P. Zotto[a,b], G. Zumerle[a,b]

INFN Sezione di Pavia[a], Università di Pavia[b], Pavia, Italy
A. Braghieri[a], A. Magnani[a], P. Montagna[a,b], S. P. Ratti[a,b], V. Re[a], M. Ressegotti[a,b], C. Riccardi[a,b], P. Salvini[a], I. Vai[a,b], P. Vitulo[a,b]

INFN Sezione di Perugia[a], Università di Perugia[b], Perugia, Italy
M. Biasini[a,b], G. M. Bilei[a], C. Cecchi[a,b], D. Ciangottini[a,b], L. Fanò[a,b], P. Lariccia[a,b], R. Leonardi[a,b], E. Manoni[a], G. Mantovani[a,b], V. Mariani[a,b], M. Menichelli[a], A. Rossi[a,b], A. Santocchia[a,b], D. Spiga[a]

INFN Sezione di Pisa[a], Università di Pisa[b], Scuola Normale Superiore di Pisa[c], Pisa, Italy
K. Androsov[a], P. Azzurri[a], G. Bagliesi[a], L. Bianchini[a], T. Boccali[a], L. Borrello, R. Castaldi[a], M. A. Ciocci[a,b],

R. Dell'Orso[a], G. Fedi[a], F. Fiori[a,c], L. Giannini[a,c], A. Giassi[a], M. T. Grippo[a], F. Ligabue[a,c], E. Manca[a,c], G. Mandorli[a,c], A. Messineo[a,b], F. Palla[a], A. Rizzi[a,b], G. Rolandi[32], P. Spagnolo[a], R. Tenchini[a], G. Tonelli[a,b], A. Venturi[a], P. G. Verdini[a]

INFN Sezione di Roma[a], Sapienza Università di Roma[b], Rome, Italy
L. Barone[a,b], F. Cavallari[a], M. Cipriani[a,b], D. Del Re[a,b], E. Di Marco[a,b], M. Diemoz[a], S. Gelli[a,b], E. Longo[a,b], B. Marzocchi[a,b], P. Meridiani[a], G. Organtini[a,b], F. Pandolfi[a], R. Paramatti[a,b], F. Preiato[a,b], S. Rahatlou[a,b], C. Rovelli[a], F. Santanastasio[a,b]

INFN Sezione di Torino[a], Università di Torino[b], Torino, Italy, Università del Piemonte Orientale[c], Novara, Italy
N. Amapane[a,b], R. Arcidiacono[a,c], S. Argiro[a,b], M. Arneodo[a,c], N. Bartosik[a], R. Bellan[a,b], C. Biino[a], A. Cappati[a,b], N. Cartiglia[a], F. Cenna[a,b], S. Cometti[a], M. Costa[a,b], R. Covarelli[a,b], N. Demaria[a], B. Kiani[a,b], C. Mariotti[a], S. Maselli[a], E. Migliore[a,b], V. Monaco[a,b], E. Monteil[a,b], M. Monteno[a], M. M. Obertino[a,b], L. Pacher[a,b], N. Pastrone[a], M. Pelliccioni[a], G. L. Pinna Angioni[a,b], A. Romero[a,b], M. Ruspa[a,c], R. Sacchi[a,b], R. Salvatico[a,b], K. Shchelina[a,b], V. Sola[a], A. Solano[a,b], D. Soldi[a,b], A. Staiano[a]

INFN Sezione di Trieste[a], Università di Trieste[b], Trieste, Italy
S. Belforte[a], V. Candelise[a,b], M. Casarsa[a], F. Cossutti[a], A. Da Rold[a,b], G. Della Ricca[a,b], F. Vazzoler[a,b], A. Zanetti[a]

Kyungpook National University, Daegu, Korea
D. H. Kim, G. N. Kim, M. S. Kim, J. Lee, S. Lee, S. W. Lee, C. S. Moon, Y. D. Oh, S. I. Pak, S. Sekmen, D. C. Son, Y. C. Yang

Chonnam National University, Institute for Universe and Elementary Particles, Kwangju, Korea
H. Kim, D. H. Moon, G. Oh

Hanyang University, Seoul, Korea
B. Francois, J. Goh[33], T. J. Kim

Korea University, Seoul, Korea
S. Cho, S. Choi, Y. Go, D. Gyun, S. Ha, B. Hong, Y. Jo, K. Lee, K. S. Lee, S. Lee, J. Lim, S. K. Park, Y. Roh

Sejong University, Seoul, Korea
H. S. Kim

Seoul National University, Seoul, Korea
J. Almond, J. Kim, J. S. Kim, H. Lee, K. Lee, K. Nam, S. B. Oh, B. C. Radburn-Smith, S. h. Seo, U. K. Yang, H. D. Yoo, G. B. Yu

University of Seoul, Seoul, Korea
D. Jeon, H. Kim, J. H. Kim, J. S. H. Lee, I. C. Park

Sungkyunkwan University, Suwon, Korea
Y. Choi, C. Hwang, J. Lee, I. Yu

Vilnius University, Vilnius, Lithuania
V. Dudenas, A. Juodagalvis, J. Vaitkus

National Centre for Particle Physics, Universiti Malaya, Kuala Lumpur, Malaysia
Z. A. Ibrahim, M. A. B. Md Ali[34], F. Mohamad Idris[35], W. A. T. Wan Abdullah, M. N. Yusli, Z. Zolkapli

Universidad de Sonora (UNISON), Hermosillo, Mexico
J. F. Benitez, A. Castaneda Hernandez, J. A. Murillo Quijada

Centro de Investigacion y de Estudios Avanzados del IPN, Mexico City, Mexico
H. Castilla-Valdez, E. De La Cruz-Burelo, M. C. Duran-Osuna, I. Heredia-De La Cruz[36], R. Lopez-Fernandez, J. Mejia Guisao, R. I. Rabadan-Trejo, M. Ramirez-Garcia, G. Ramirez-Sanchez, R. Reyes-Almanza, A. Sanchez-Hernandez

Universidad Iberoamericana, Mexico City, Mexico
S. Carrillo Moreno, C. Oropeza Barrera, F. Vazquez Valencia

Benemerita Universidad Autonoma de Puebla, Puebla, Mexico
J. Eysermans, I. Pedraza, H. A. Salazar Ibarguen, C. Uribe Estrada

Universidad Autónoma de San Luis Potosí, San Luis Potosí, Mexico
A. Morelos Pineda

University of Auckland, Auckland, New Zealand
D. Krofcheck

University of Canterbury, Christchurch, New Zealand
S. Bheesette, P. H. Butler

National Centre for Physics, Quaid-I-Azam University, Islamabad, Pakistan
A. Ahmad, M. Ahmad, M. I. Asghar, Q. Hassan, H. R. Hoorani, W. A. Khan, M. A. Shah, M. Shoaib, M. Waqas

National Centre for Nuclear Research, Swierk, Poland
H. Bialkowska, M. Bluj, B. Boimska, T. Frueboes, M. Górski, M. Kazana, M. Szleper, P. Traczyk, P. Zalewski

Institute of Experimental Physics, Faculty of Physics, University of Warsaw, Warsaw, Poland
K. Bunkowski, A. Byszuk[37], K. Doroba, A. Kalinowski, M. Konecki, J. Krolikowski, M. Misiura, M. Olszewski, A. Pyskir, M. Walczak

Laboratório de Instrumentação e Física Experimental de Partículas, Lisboa, Portugal
M. Araujo, P. Bargassa, C. Beirão Da CruzE Silva, A. Di Francesco, P. Faccioli, B. Galinhas, M. Gallinaro, J. Hollar, N. Leonardo, J. Seixas, G. Strong, O. Toldaiev, J. Varela

Joint Institute for Nuclear Research, Dubna, Russia
S. Afanasiev, P. Bunin, M. Gavrilenko, I. Golutvin, I. Gorbunov, A. Kamenev, V. Karjavine, A. Lanev, A. Malakhov, V. Matveev[38,39], P. Moisenz, V. Palichik, V. Perelygin, S. Shmatov, S. Shulha, N. Skatchkov, V. Smirnov, N. Voytishin, A. Zarubin

Petersburg Nuclear Physics Institute, Gatchina (St. Petersburg), Russia
V. Golovtsov, Y. Ivanov, V. Kim[40], E. Kuznetsova[41], P. Levchenko, V. Murzin, V. Oreshkin, I. Smirnov, D. Sosnov, V. Sulimov, L. Uvarov, S. Vavilov, A. Vorobyev

Institute for Nuclear Research, Moscow, Russia
Yu. Andreev, A. Dermenev, S. Gninenko, N. Golubev, A. Karneyeu, M. Kirsanov, N. Krasnikov, A. Pashenkov, A. Shabanov, D. Tlisov, A. Toropin

Institute for Theoretical and Experimental Physics, Moscow, Russia
V. Epshteyn, V. Gavrilov, N. Lychkovskaya, V. Popov, I. Pozdnyakov, G. Safronov, A. Spiridonov, A. Stepennov, V. Stolin, M. Toms, E. Vlasov, A. Zhokin

Moscow Institute of Physics and Technology, Moscow, Russia
T. Aushev

National Research Nuclear University 'Moscow Engineering Physics Institute' (MEPhI), Moscow, Russia
M. Chadeeva[42], D. Philippov, E. Popova, V. Rusinov

P.N. Lebedev Physical Institute, Moscow, Russia
V. Andreev, M. Azarkin, I. Dremin[39], M. Kirakosyan, A. Terkulov

Skobeltsyn Institute of Nuclear Physics, Lomonosov Moscow State University, Moscow, Russia
A. Belyaev, E. Boos, M. Dubinin[43], L. Dudko, A. Ershov, A. Gribushin, V. Klyukhin, O. Kodolova, I. Lokhtin, S. Obraztsov, S. Petrushanko, V. Savrin, A. Snigirev

Novosibirsk State University (NSU), Novosibirsk, Russia
A. Barnyakov[44], V. Blinov[44], T. Dimova[44], L. Kardapoltsev[44], Y. Skovpen[44]

Institute for High Energy Physics of National Research Centre 'Kurchatov Institute', Protvino, Russia
I. Azhgirey, I. Bayshev, S. Bitioukov, V. Kachanov, A. Kalinin, D. Konstantinov, P. Mandrik, V. Petrov, R. Ryutin, S. Slabospitskii, A. Sobol, S. Troshin, N. Tyurin, A. Uzunian, A. Volkov

National Research Tomsk Polytechnic University, Tomsk, Russia
A. Babaev, S. Baidali, V. Okhotnikov

University of Belgrade, Faculty of Physics and Vinca Institute of Nuclear Sciences, Belgrade, Serbia
P. Adzic[45], P. Cirkovic, D. Devetak, M. Dordevic, J. Milosevic

Centro de Investigaciones Energéticas Medioambientales y Tecnológicas (CIEMAT), Madrid, Spain
J. Alcaraz Maestre, A. Álvarez Fernández, I. Bachiller, M. Barrio Luna, J. A. Brochero Cifuentes, M. Cerrada, N. Colino, B. De La Cruz, A. Delgado Peris, C. Fernandez Bedoya, J. P. Fernández Ramos, J. Flix, M. C. Fouz, O. Gonzalez Lopez, S. Goy Lopez, J. M. Hernandez, M. I. Josa, D. Moran, A. Pérez-Calero Yzquierdo, J. Puerta Pelayo, I. Redondo, L. Romero, S. Sánchez Navas, M. S. Soares, A. Triossi

Universidad Autónoma de Madrid, Madrid, Spain
C. Albajar, J. F. de Trocóniz

Universidad de Oviedo, Oviedo, Spain
J. Cuevas, C. Erice, J. Fernandez Menendez, S. Folgueras, I. Gonzalez Caballero, J. R. González Fernández, E. Palencia Cortezon, V. Rodríguez Bouza, S. Sanchez Cruz, J. M. Vizan Garcia

Instituto de Física de Cantabria (IFCA), CSIC-Universidad de Cantabria, Santander, Spain
I. J. Cabrillo, A. Calderon, B. Chazin Quero, J. Duarte Campderros, M. Fernandez, P. J. Fernández Manteca, A. García Alonso, J. Garcia-Ferrero, G. Gomez, A. Lopez Virto, J. Marco, C. Martinez Rivero, P. Martinez Ruiz del Arbol, F. Matorras, J. Piedra Gomez, C. Prieels, T. Rodrigo, A. Ruiz-Jimeno, L. Scodellaro, N. Trevisani, I. Vila, R. Vilar Cortabitarte

Department of Physics, University of Ruhuna, Matara, Sri Lanka
N. Wickramage

CERN, European Organization for Nuclear Research, Geneva, Switzerland
D. Abbaneo, B. Akgun, E. Auffray, G. Auzinger, P. Baillon, A. H. Ball, D. Barney, J. Bendavid, M. Bianco, A. Bocci, C. Botta, E. Brondolin, T. Camporesi, M. Cepeda, G. Cerminara, E. Chapon, Y. Chen, G. Cucciati, D. d'Enterria, A. Dabrowski, N. Daci, V. Daponte, A. David, A. De Roeck, N. Deelen, M. Dobson, M. Dünser, N. Dupont, A. Elliott-Peisert, P. Everaerts, F. Fallavollita[46], D. Fasanella, G. Franzoni, J. Fulcher, W. Funk, D. Gigi, A. Gilbert, K. Gill, F. Glege, M. Gruchala, M. Guilbaud, D. Gulhan, J. Hegeman, C. Heidegger, V. Innocente, A. Jafari, P. Janot, O. Karacheban[20], J. Kieseler, A. Kornmayer, M. Krammer[1], C. Lange, P. Lecoq, C. Lourenço, L. Malgeri, M. Mannelli, A. Massironi, F. Meijers, J. A. Merlin, S. Mersi, E. Meschi, P. Milenovic[47], F. Moortgat, M. Mulders, J. Ngadiuba, S. Nourbakhsh, S. Orfanelli, L. Orsini, F. Pantaleo[17], L. Pape, E. Perez, M. Peruzzi, A. Petrilli, G. Petrucciani, A. Pfeiffer, M. Pierini, F. M. Pitters, D. Rabady, A. Racz, T. Reis, M. Rovere, H. Sakulin, C. Schäfer, C. Schwick, M. Selvaggi, A. Sharma, P. Silva, P. Sphicas[48], A. Stakia, J. Steggemann, D. Treille, A. Tsirou, A. Vartak, V. Veckalns[49], M. Verzetti, W. D. Zeuner

Paul Scherrer Institut, Villigen, Switzerland
L. Caminada[50], K. Deiters, W. Erdmann, R. Horisberger, Q. Ingram, H. C. Kaestli, D. Kotlinski, U. Langenegger, T. Rohe, S. A. Wiederkehr

ETH Zurich - Institute for Particle Physics and Astrophysics (IPA), Zurich, Switzerland
M. Backhaus, L. Bäni, P. Berger, N. Chernyavskaya, G. Dissertori, M. Dittmar, M. Donegà, C. Dorfer, T. A. Gómez Espinosa, C. Grab, D. Hits, T. Klijnsma, W. Lustermann, R. A. Manzoni, M. Marionneau, M. T. Meinhard, F. Micheli, P. Musella, F. Nessi-Tedaldi, F. Pauss, G. Perrin, L. Perrozzi, S. Pigazzini, C. Reissel, D. Ruini, D. A. Sanz Becerra, M. Schönenberger, L. Shchutska, V. R. Tavolaro, K. Theofilatos, M. L. Vesterbacka Olsson, R. Wallny, D. H. Zhu

Universität Zürich, Zurich, Switzerland
T. K. Aarrestad, C. Amsler[51], D. Brzhechko, M. F. Canelli, A. De Cosa, R. Del Burgo, S. Donato, C. Galloni, T. Hreus,

B. Kilminster, S. Leontsinis, I. Neutelings, G. Rauco, P. Robmann, D. Salerno, K. Schweiger, C. Seitz, Y. Takahashi, A. Zucchetta

National Central University, Chung-Li, Taiwan
T. H. Doan, R. Khurana, C. M. Kuo, W. Lin, A. Pozdnyakov, S. S. Yu

National Taiwan University (NTU), Taipei, Taiwan
P. Chang, Y. Chao, K. F. Chen, P. H. Chen, W.-S. Hou, Y. F. Liu, R.-S. Lu, E. Paganis, A. Psallidas, A. Steen

Faculty of Science, Department of Physics, Chulalongkorn University, Bangkok, Thailand
B. Asavapibhop, N. Srimanobhas, N. Suwonjandee

Physics Department, Science and Art Faculty, Çukurova University, Adana, Turkey
M. N. Bakirci[52], A. Bat, F. Boran, S. Damarseckin, Z. S. Demiroglu, F. Dolek, C. Dozen, I. Dumanoglu, G. Gokbulut, Y. Guler, E. Gurpinar, I. Hos[53], C. Isik, E. E. Kangal[54], O. Kara, A. Kayis Topaksu, U. Kiminsu, M. Oglakci, G. Onengut, K. Ozdemir[55], S. Ozturk[52], B. Tali[56], U. G. Tok, H. Topakli[52], S. Turkcapar, I. S. Zorbakir, C. Zorbilmez

Physics Department, Middle East Technical University, Ankara, Turkey
B. Isildak[57], G. Karapinar[58], M. Yalvac, M. Zeyrek

Bogazici University, Istanbul, Turkey
I. O. Atakisi, E. Gülmez, M. Kaya[59], O. Kaya[60], S. Ozkorucuklu[61], S. Tekten, E. A. Yetkin[62]

Istanbul Technical University, Istanbul, Turkey
M. N. Agaras, A. Cakir, K. Cankocak, Y. Komurcu, S. Sen[63]

Institute for Scintillation Materials of National Academy of Science of Ukraine, Kharkov, Ukraine
B. Grynyov

National Scientific Center, Kharkov Institute of Physics and Technology, Kharkov, Ukraine
L. Levchuk

University of Bristol, Bristol, UK
F. Ball, J. J. Brooke, D. Burns, E. Clement, D. Cussans, O. Davignon, H. Flacher, J. Goldstein, G. P. Heath, H. F. Heath, L. Kreczko, D. M. Newbold[64], S. Paramesvaran, B. Penning, T. Sakuma, D. Smith, V. J. Smith, J. Taylor, A. Titterton

Rutherford Appleton Laboratory, Didcot, UK
K. W. Bell, A. Belyaev[65], C. Brew, R. M. Brown, D. Cieri, D. J. A. Cockerill, J. A. Coughlan, K. Harder, S. Harper, J. Linacre, K. Manolopoulos, E. Olaiya, D. Petyt, C. H. Shepherd-Themistocleous, A. Thea, I. R. Tomalin, T. Williams, W. J. Womersley

Imperial College, London, UK
R. Bainbridge, P. Bloch, J. Borg, S. Breeze, O. Buchmuller, A. Bundock, D. Colling, P. Dauncey, G. Davies, M. Della Negra, R. Di Maria, G. Hall, G. Iles, T. James, M. Komm, C. Laner, L. Lyons, A.-M. Magnan, S. Malik, A. Martelli, J. Nash[66], A. Nikitenko[7], V. Palladino, M. Pesaresi, D. M. Raymond, A. Richards, A. Rose, E. Scott, C. Seez, A. Shtipliyski, G. Singh, M. Stoye, T. Strebler, S. Summers, A. Tapper, K. Uchida, T. Virdee[17], N. Wardle, D. Winterbottom, J. Wright, S. C. Zenz

Brunel University, Uxbridge, UK
J. E. Cole, P. R. Hobson, A. Khan, P. Kyberd, C. K. Mackay, A. Morton, I. D. Reid, L. Teodorescu, S. Zahid

Baylor University, Waco, USA
K. Call, J. Dittmann, K. Hatakeyama, H. Liu, C. Madrid, B. McMaster, N. Pastika, C. Smith

Catholic University of America, Washington, DC, USA
R. Bartek, A. Dominguez

The University of Alabama, Tuscaloosa, USA
A. Buccilli, S. I. Cooper, C. Henderson, P. Rumerio, C. West

Boston University, Boston, USA
D. Arcaro, T. Bose, D. Gastler, S. Girgis, D. Pinna, C. Richardson, J. Rohlf, L. Sulak, D. Zou

Brown University, Providence, USA
G. Benelli, B. Burkle, X. Coubez, D. Cutts, M. Hadley, J. Hakala, U. Heintz, J. M. Hogan[67], K. H. M. Kwok, E. Laird, G. Landsberg, J. Lee, Z. Mao, M. Narain, S. Sagir[68], R. Syarif, E. Usai, D. Yu

University of California, Davis, Davis, USA
R. Band, C. Brainerd, R. Breedon, D. Burns, M. Calderon De La Barca Sanchez, M. Chertok, J. Conway, R. Conway, P. T. Cox, R. Erbacher, C. Flores, G. Funk, W. Ko, O. Kukral, R. Lander, M. Mulhearn, D. Pellett, J. Pilot, S. Shalhout, M. Shi, D. Stolp, D. Taylor, K. Tos, M. Tripathi, Z. Wang, F. Zhang

University of California, Los Angeles, USA
M. Bachtis, C. Bravo, R. Cousins, A. Dasgupta, S Erhan, A. Florent, J. Hauser, M. Ignatenko, N. Mccoll, S. Regnard, D. Saltzberg, C. Schnaible, V. Valuev

University of California, Riverside, Riverside, USA
E. Bouvier, K. Burt, R. Clare, J. W. Gary, S. M. A. Ghiasi Shirazi, G. Hanson, G. Karapostoli, E. Kennedy, F. Lacroix, O. R. Long, M. Olmedo Negrete, M. I. Paneva, W. Si, L. Wang, H. Wei, S. Wimpenny, B. R. Yates

University of California, San Diego, La Jolla, USA
J. G. Branson, P. Chang, S. Cittolin, M. Derdzinski, R. Gerosa, D. Gilbert, B. Hashemi, A. Holzner, D. Klein, G. Kole, V. Krutelyov, J. Letts, M. Masciovecchio, S. May, D. Olivito, S. Padhi, M. Pieri, V. Sharma, M. Tadel, J. Wood, F. Würthwein, A. Yagil, G. Zevi Della Porta

Department of Physics, University of California, Santa Barbara, Santa Barbara, USA
N. Amin, R. Bhandari, C. Campagnari, M. Citron, V. Dutta, M. Franco Sevilla, L. Gouskos, R. Heller, J. Incandela, H. Mei, A. Ovcharova, H. Qu, J. Richman, D. Stuart, I. Suarez, S. Wang, J. Yoo

California Institute of Technology, Pasadena, USA
D. Anderson, A. Bornheim, J. M. Lawhorn, N. Lu, H. B. Newman, T. Q. Nguyen, J. Pata, M. Spiropulu, J. R. Vlimant, R. Wilkinson, S. Xie, Z. Zhang, R. Y. Zhu

Carnegie Mellon University, Pittsburgh, USA
M. B. Andrews, T. Ferguson, T. Mudholkar, M. Paulini, M. Sun, I. Vorobiev, M. Weinberg

University of Colorado Boulder, Boulder, USA
J. P. Cumalat, W. T. Ford, F. Jensen, A. Johnson, E. MacDonald, T. Mulholland, R. Patel, A. Perloff, K. Stenson, K. A. Ulmer, S. R. Wagner

Cornell University, Ithaca, USA
J. Alexander, J. Chaves, Y. Cheng, J. Chu, A. Datta, K. Mcdermott, N. Mirman, J. R. Patterson, D. Quach, A. Rinkevicius, A. Ryd, L. Skinnari, L. Soffi, S. M. Tan, Z. Tao, J. Thom, J. Tucker, P. Wittich, M. Zientek

Fermi National Accelerator Laboratory, Batavia, USA
S. Abdullin, M. Albrow, M. Alyari, G. Apollinari, A. Apresyan, A. Apyan, S. Banerjee, L. A. T. Bauerdick, A. Beretvas, J. Berryhill, P. C. Bhat, K. Burkett, J. N. Butler, A. Canepa, G. B. Cerati, H. W. K. Cheung, F. Chlebana, M. Cremonesi, J. Duarte, V. D. Elvira, J. Freeman, Z. Gecse, E. Gottschalk, L. Gray, D. Green, S. Grünendahl, O. Gutsche, J. Hanlon, R. M. Harris, S. Hasegawa, J. Hirschauer, Z. Hu, B. Jayatilaka, S. Jindariani, M. Johnson, U. Joshi, B. Klima, M. J. Kortelainen, B. Kreis, S. Lammel, D. Lincoln, R. Lipton, M. Liu, T. Liu, J. Lykken, K. Maeshima, J. M. Marraffino, D. Mason, P. McBride, P. Merkel, S. Mrenna, S. Nahn, V. O'Dell, K. Pedro, C. Pena, O. Prokofyev, G. Rakness, F. Ravera, A. Reinsvold, L. Ristori, A. Savoy-Navarro[69], B. Schneider, E. Sexton-Kennedy, A. Soha, W. J. Spalding, L. Spiegel, S. Stoynev, J. Strait, N. Strobbe, L. Taylor, S. Tkaczyk, N. V. Tran, L. Uplegger, E. W. Vaandering, C. Vernieri, M. Verzocchi, R. Vidal, M. Wang, H. A. Weber, A. Whitbeck

University of Florida, Gainesville, USA
D. Acosta, P. Avery, P. Bortignon, D. Bourilkov, A. Brinkerhoff, L. Cadamuro, A. Carnes, D. Curry, R. D. Field, S. V. Gleyzer, B. M. Joshi, J. Konigsberg, A. Korytov, K. H. Lo, P. Ma, K. Matchev, G. Mitselmakher, D. Rosenzweig, K. Shi, D. Sperka, J. Wang, S. Wang, X. Zuo

Florida International University, Miami, USA
Y. R. Joshi, S. Linn

Florida State University, Tallahassee, USA
A. Ackert, T. Adams, A. Askew, S. Hagopian, V. Hagopian, K. F. Johnson, T. Kolberg, G. Martinez, T. Perry, H. Prosper, A. Saha, C. Schiber, R. Yohay

Florida Institute of Technology, Melbourne, USA
M. M. Baarmand, V. Bhopatkar, S. Colafranceschi, M. Hohlmann, D. Noonan, M. Rahmani, T. Roy, M. Saunders, F. Yumiceva

University of Illinois at Chicago (UIC), Chicago, USA
M. R. Adams, L. Apanasevich, D. Berry, R. R. Betts, R. Cavanaugh, X. Chen, S. Dittmer, O. Evdokimov, C. E. Gerber, D. A. Hangal, D. J. Hofman, K. Jung, J. Kamin, C. Mills, M. B. Tonjes, N. Varelas, H. Wang, X. Wang, Z. Wu, J. Zhang

The University of Iowa, Iowa City, USA
M. Alhusseini, B. Bilki[70], W. Clarida, K. Dilsiz[71], S. Durgut, R. P. Gandrajula, M. Haytmyradov, V. Khristenko, J.-P. Merlo, A. Mestvirishvili, A. Moeller, J. Nachtman, H. Ogul[72], Y. Onel, F. Ozok[73], A. Penzo, C. Snyder, E. Tiras, J. Wetzel

Johns Hopkins University, Baltimore, USA
B. Blumenfeld, A. Cocoros, N. Eminizer, D. Fehling, L. Feng, A. V. Gritsan, W. T. Hung, P. Maksimovic, J. Roskes, U. Sarica, M. Swartz, M. Xiao

The University of Kansas, Lawrence, USA
A. Al-bataineh, P. Baringer, A. Bean, S. Boren, J. Bowen, A. Bylinkin, J. Castle, S. Khalil, A. Kropivnitskaya, D. Majumder, W. Mcbrayer, M. Murray, C. Rogan, S. Sanders, E. Schmitz, J. D. Tapia Takaki, Q. Wang

Kansas State University, Manhattan, USA
S. Duric, A. Ivanov, K. Kaadze, D. Kim, Y. Maravin, D. R. Mendis, T. Mitchell, A. Modak, A. Mohammadi

Lawrence Livermore National Laboratory, Livermore, USA
F. Rebassoo, D. Wright

University of Maryland, College Park, USA
A. Baden, O. Baron, A. Belloni, S. C. Eno, Y. Feng, C. Ferraioli, N. J. Hadley, S. Jabeen, G. Y. Jeng, R. G. Kellogg, J. Kunkle, A. C. Mignerey, S. Nabili, F. Ricci-Tam, M. Seidel, Y. H. Shin, A. Skuja, S. C. Tonwar, K. Wong

Massachusetts Institute of Technology, Cambridge, USA
D. Abercrombie, B. Allen, V. Azzolini, A. Baty, G. Bauer, R. Bi, S. Brandt, W. Busza, I. A. Cali, M. D'Alfonso, Z. Demiragli, G. Gomez Ceballos, M. Goncharov, P. Harris, D. Hsu, M. Hu, Y. Iiyama, G. M. Innocenti, M. Klute, D. Kovalskyi, Y.-J. Lee, P. D. Luckey, B. Maier, A. C. Marini, C. Mcginn, C. Mironov, S. Narayanan, X. Niu, C. Paus, D. Rankin, C. Roland, G. Roland, Z. Shi, G. S. F. Stephans, K. Sumorok, K. Tatar, D. Velicanu, J. Wang, T. W. Wang, B. Wyslouch

University of Minnesota, Minneapolis, USA
A. C. Benvenuti[†], R. M. Chatterjee, A. Evans, P. Hansen, J. Hiltbrand, Sh. Jain, S. Kalafut, M. Krohn, Y. Kubota, Z. Lesko, J. Mans, R. Rusack, M. A. Wadud

University of Mississippi, Oxford, USA
J. G. Acosta, S. Oliveros

University of Nebraska-Lincoln, Lincoln, USA
E. Avdeeva, K. Bloom, D. R. Claes, C. Fangmeier, F. Golf, R. Gonzalez Suarez, R. Kamalieddin, I. Kravchenko, J. Monroy, J. E. Siado, G. R. Snow, B. Stieger

State University of New York at Buffalo, Buffalo, USA
A. Godshalk, C. Harrington, I. Iashvili, A. Kharchilava, C. Mclean, D. Nguyen, A. Parker, S. Rappoccio, B. Roozbahani

Northeastern University, Boston, USA
G. Alverson, E. Barberis, C. Freer, Y. Haddad, A. Hortiangtham, G. Madigan, D. M. Morse, T. Orimoto, A. Tishelman-charny, T. Wamorkar, B. Wang, A. Wisecarver, D. Wood

Northwestern University, Evanston, USA
S. Bhattacharya, J. Bueghly, O. Charaf, T. Gunter, K. A. Hahn, N. Odell, M. H. Schmitt, K. Sung, M. Trovato, M. Velasco

University of Notre Dame, Notre Dame, USA
R. Bucci, N. Dev, M. Hildreth, K. Hurtado Anampa, C. Jessop, D. J. Karmgard, K. Lannon, W. Li, N. Loukas, N. Marinelli, F. Meng, C. Mueller, Y. Musienko[38], M. Planer, R. Ruchti, P. Siddireddy, G. Smith, S. Taroni, M. Wayne, A. Wightman, M. Wolf, A. Woodard

The Ohio State University, Columbus, USA
J. Alimena, L. Antonelli, B. Bylsma, L. S. Durkin, S. Flowers, B. Francis, C. Hill, W. Ji, T. Y. Ling, W. Luo, B. L. Winer

Princeton University, Princeton, USA
S. Cooperstein, P. Elmer, J. Hardenbrook, N. Haubrich, S. Higginbotham, A. Kalogeropoulos, S. Kwan, D. Lange, M. T. Lucchini, J. Luo, D. Marlow, K. Mei, I. Ojalvo, J. Olsen, C. Palmer, P. Piroué, J. Salfeld-Nebgen, D. Stickland, C. Tully

University of Puerto Rico, Mayaguez, USA
S. Malik, S. Norberg

Purdue University, West Lafayette, USA
A. Barker, V. E. Barnes, S. Das, L. Gutay, M. Jones, A. W. Jung, A. Khatiwada, B. Mahakud, D. H. Miller, N. Neumeister, C. C. Peng, S. Piperov, H. Qiu, J. F. Schulte, J. Sun, F. Wang, R. Xiao, W. Xie

Purdue University Northwest, Hammond, USA
T. Cheng, J. Dolen, N. Parashar

Rice University, Houston, USA
Z. Chen, K. M. Ecklund, S. Freed, F. J. M. Geurts, M. Kilpatrick, Arun Kumar, W. Li, B. P. Padley, R. Redjimi, J. Roberts, J. Rorie, W. Shi, Z. Tu, A. Zhang

University of Rochester, Rochester, USA
A. Bodek, P. de Barbaro, R. Demina, Y. t. Duh, J. L. Dulemba, C. Fallon, T. Ferbel, M. Galanti, A. Garcia-Bellido, J. Han, O. Hindrichs, A. Khukhunaishvili, E. Ranken, P. Tan, R. Taus

Rutgers, The State University of New Jersey, Piscataway, USA
B. Chiarito, J. P. Chou, Y. Gershtein, E. Halkiadakis, A. Hart, M. Heindl, E. Hughes, S. Kaplan, R. Kunnawalkam Elayavalli, S. Kyriacou, I. Laflotte, A. Lath, R. Montalvo, K. Nash, M. Osherson, H. Saka, S. Salur, S. Schnetzer, D. Sheffield, S. Somalwar, R. Stone, S. Thomas, P. Thomassen

University of Tennessee, Knoxville, USA
A. G. Delannoy, J. Heideman, G. Riley, S. Spanier

Texas A&M University, College Station, USA
O. Bouhali[74], A. Celik, M. Dalchenko, M. De Mattia, A. Delgado, S. Dildick, R. Eusebi, J. Gilmore, T. Huang, T. Kamon[75], S. Luo, D. Marley, R. Mueller, D. Overton, L. Perniè, D. Rathjens, A. Safonov

Texas Tech University, Lubbock, USA
N. Akchurin, J. Damgov, F. De Guio, P. R. Dudero, S. Kunori, K. Lamichhane, S. W. Lee, T. Mengke, S. Muthumuni, T. Peltola, S. Undleeb, I. Volobouev, Z. Wang

Vanderbilt University, Nashville, USA
S. Greene, A. Gurrola, R. Janjam, W. Johns, C. Maguire, A. Melo, H. Ni, K. Padeken, F. Romeo, J. D. Ruiz Alvarez, P. Sheldon, S. Tuo, J. Velkovska, M. Verweij, Q. Xu

University of Virginia, Charlottesville, USA
M. W. Arenton, P. Barria, B. Cox, R. Hirosky, M. Joyce, A. Ledovskoy, H. Li, C. Neu, T. Sinthuprasith, Y. Wang, E. Wolfe, F. Xia

Wayne State University, Detroit, USA
R. Harr, P. E. Karchin, N. Poudyal, J. Sturdy, P. Thapa, S. Zaleski

University of Wisconsin - Madison, Madison, WI, USA
J. Buchanan, C. Caillol, D. Carlsmith, S. Dasu, I. De Bruyn, L. Dodd, B. Gomber[76], M. Grothe, M. Herndon, A. Hervé, U. Hussain, P. Klabbers, A. Lanaro, K. Long, R. Loveless, T. Ruggles, A. Savin, V. Sharma, N. Smith, W. H. Smith, N. Woods

† **Deceased**

1: Also at Vienna University of Technology, Vienna, Austria
2: Also at IRFU, CEA, Université Paris-Saclay, Gif-sur-Yvette, France
3: Also at Universidade Estadual de Campinas, Campinas, Brazil
4: Also at Federal University of Rio Grande do Sul, Porto Alegre, Brazil
5: Also at Université Libre de Bruxelles, Bruxelles, Belgium
6: Also at University of Chinese Academy of Sciences, Beijing, China
7: Also at Institute for Theoretical and Experimental Physics, Moscow, Russia
8: Also at Joint Institute for Nuclear Research, Dubna, Russia
9: Now at Cairo University, Cairo, Egypt
10: Also at Zewail City of Science and Technology, Zewail, Egypt
11: Also at British University in Egypt, Cairo, Egypt
12: Now at Ain Shams University, Cairo, Egypt
13: Also at Department of Physics, King Abdulaziz University, Jeddah, Saudi Arabia
14: Also at Université de Haute Alsace, Mulhouse, France
15: Also at Skobeltsyn Institute of Nuclear Physics, Lomonosov Moscow State University, Moscow, Russia
16: Also at Tbilisi State University, Tbilisi, Georgia
17: Also at CERN, European Organization for Nuclear Research, Geneva, Switzerland
18: Also at RWTH Aachen University, III. Physikalisches Institut A, Aachen, Germany
19: Also at University of Hamburg, Hamburg, Germany
20: Also at Brandenburg University of Technology, Cottbus, Germany
21: Also at Institute of Physics, University of Debrecen, Debrecen, Hungary
22: Also at Institute of Nuclear Research ATOMKI, Debrecen, Hungary
23: Also at MTA-ELTE Lendület CMS Particle and Nuclear Physics Group, Eötvös Loránd University, Budapest, Hungary
24: Also at Indian Institute of Technology Bhubaneswar, Bhubaneswar, India
25: Also at Institute of Physics, Bhubaneswar, India
26: Also at Shoolini University, Solan, India
27: Also at University of Visva-Bharati, Santiniketan, India
28: Also at Isfahan University of Technology, Isfahan, Iran
29: Also at Plasma Physics Research Center, Science and Research Branch, Islamic Azad University, Tehran, Iran
30: Also at ITALIAN NATIONAL AGENCY FOR NEW TECHNOLOGIES, ENERGY AND SUSTAINABLE ECONOMIC DEVELOPMENT, Bologna, Italy
31: Also at Università degli Studi di Siena, Siena, Italy
32: Also at Scuola Normale e Sezione dell'INFN, Pisa, Italy
33: Also at Kyunghee University, Seoul, Korea
34: Also at International Islamic University of Malaysia, Kuala Lumpur, Malaysia
35: Also at Malaysian Nuclear Agency, MOSTI, Kajang, Malaysia
36: Also at Consejo Nacional de Ciencia y Tecnología, Mexico City, Mexico
37: Also at Warsaw University of Technology, Institute of Electronic Systems, Warsaw, Poland
38: Also at Institute for Nuclear Research, Moscow, Russia
39: Now at National Research Nuclear University 'Moscow Engineering Physics Institute' (MEPhI), Moscow, Russia
40: Also at St. Petersburg State Polytechnical University, St. Petersburg, Russia

41: Also at University of Florida, Gainesville, USA
42: Also at P.N. Lebedev Physical Institute, Moscow, Russia
43: Also at California Institute of Technology, Pasadena, USA
44: Also at Budker Institute of Nuclear Physics, Novosibirsk, Russia
45: Also at Faculty of Physics, University of Belgrade, Belgrade, Serbia
46: Also at INFN Sezione di Pavia [a], Università di Pavia [b], Pavia, Italy
47: Also at University of Belgrade, Faculty of Physics and Vinca Institute of Nuclear Sciences, Belgrade, Serbia
48: Also at National and Kapodistrian University of Athens, Athens, Greece
49: Also at Riga Technical University, Riga, Latvia
50: Also at Universität Zürich, Zurich, Switzerland
51: Also at Stefan Meyer Institute for Subatomic Physics (SMI), Vienna, Austria
52: Also at Gaziosmanpasa University, Tokat, Turkey
53: Also at Istanbul Aydin University, Istanbul, Turkey
54: Also at Mersin University, Mersin, Turkey
55: Also at Piri Reis University, Istanbul, Turkey
56: Also at Adiyaman University, Adiyaman, Turkey
57: Also at Ozyegin University, Istanbul, Turkey
58: Also at Izmir Institute of Technology, Izmir, Turkey
59: Also at Marmara University, Istanbul, Turkey
60: Also at Kafkas University, Kars, Turkey
61: Also at Istanbul University, Faculty of Science, Istanbul, Turkey
62: Also at Istanbul Bilgi University, Istanbul, Turkey
63: Also at Hacettepe University, Ankara, Turkey
64: Also at Rutherford Appleton Laboratory, Didcot, United Kingdom
65: Also at School of Physics and Astronomy, University of Southampton, Southampton, United Kingdom
66: Also at Monash University, Faculty of Science, Clayton, Australia
67: Also at Bethel University, St. Paul, USA
68: Also at Karamanoğlu Mehmetbey University, Karaman, Turkey
69: Also at Purdue University, West Lafayette, USA
70: Also at Beykent University, Istanbul, Turkey
71: Also at Bingol University, Bingol, Turkey
72: Also at Sinop University, Sinop, Turkey
73: Also at Mimar Sinan University, Istanbul, Istanbul, Turkey
74: Also at Texas A&M University at Qatar, Doha, Qatar
75: Also at Kyungpook National University, Daegu, Korea
76: Also at University of Hyderabad, Hyderabad, India